New Journal of Chemistry

Synthesis, structural, biological and *in silico* studies of some new 5-arylidene-4-thiazolidinone derivatives as possible anticancer, antimicrobial and antitubercular agents

Sunil Kumar. A[a], Jyothi Kudva[a,*], Bharath. B. R[b], Ananda K[c], Rajitha Sadashiva[d], Madan Kumar. S[e], Revanasiddappa. B. C[f], Vasantha Kumar[g], Rekha. P. D[h].

[a]*Department of Chemistry, St Joseph Engineering College, Mangaluru, 575028, India.*
[b]*Department of Biotechnology, NMAM Institute of Technology, Nitte- 574110, India.*
[c]*Biological Sciences, Poornaprajna Institute of Scientific Research, Devanahalli, Bangalore-562 164, India.*
[d]*Sigma-Aldrich Chemical Pvt. Ltd, Bengaluru, India*
[e]*DST-PURSE Lab, Mangalagangotri, Mangalore University, Mangaluru, 574199, India.*
[f]*Department of Pharmaceutical Chemistry, NGSM Institute of Pharmaceutical Sciences, Nitte University, Paneer, Mangaluru-575018, India.*
[g]*Department of Chemistry, Sri Dharmasthala Manjunatheshwara College (Autonomous) Ujire-574240, India.*
[h]*Yenepoya Research Centre, Yenepoya University, Mangaluru- 575018, India.*

[*]*Corresponding author's email: jyothikudva@gmail.com*

Electronic Supplementary Information

Supplementary data contain procedure for the biological studies and molecular docking scanned spectra of selected compounds.

In vitro anticancer activity

The *in vitro* cytotoxic activity of newly synthesized compounds was tested on human breast cancer cell line, MDA-MB-231. The cell lines were procured from NCC Pune, India. The activity was tested by MTT assay method and the experiment was carried out at Department of Microbiology, Yenepoya University, Karnataka, India. MDA-MB-231 cells were seeded onto a 96 well titer plate containing DMEM High Glucose H-21 media supplemented with 10 % FBS (Fetal Bovine Serum), containing Penicillin-Streptomycin and L-Glutamine, at a seeding density of 5×10^3 cells/well and incubated at 37 ^oC and 5 % CO_2 for 12 h. The test compounds were

dissolved in a minimum concentration of DMSO and added to the wells at a concentration of 50 µM and incubated for 48 h. MTT solution was prepared by dissolving 5 mg/mL of PBS buffer and added 20 µL to each well after 48 h and further incubated for 4 h. The media was removed and DMSO (100 µL) was added to the well to dissolve the reduced formazan crystals. The absorbance was recorded at 570 nm (FluoSTAR Omega, BMG Labtech). The highest cell killing activity showing compounds based on the above experiment were further selected to find out its IC_{50} values. Five different concentrations (10, 20, 30, 40 and 50 µM) of the compounds were prepared and the experiment was carried out by MTT assay method. Cisplatin was used as the reference drug. The percentage growth inhibition was calculated using the following formula,

% Cell inhibition = 100-{[(At-Ab)/(Ac-Ab)]x100}

Where, At= Absorbance value of test compound, Ab= Absorbance value of blank and Ac =Absorbance value of the control.

***In vitro* antibacterial activity**

The antibacterial activity was performed by disc diffusion method. Brain Heart Infusion agar was used as medium and the samples were tested at 100 µg/mL concentration. Ciprofloxacin was used as reference standard drug and DMSO as a solvent control. The bacterial colonies were transferred to the plates and the inoculums were prepared by adjusting the turbidity to a McFarland 0.5 turbidity standard. The wells were prepared by pressing a heated hollow tube of diameter 5 mm on an inoculated agar plate. The compounds were tested with 50 µg/mL concentration. 50 µL of each compound is applied to the respective wells and incubated for 18-24 h at 37 ^{o}C. The inhibition zone was measured in millimetre by holding the measuring device.

***In vitro* antifungal activity**

The antifungal activity was also carried out by disc diffusion method as described above. In this method, Sabouraud agar was used as a medium instead of Brain heart infusion agar and Fluconazole as a reference drug. The compounds were tested with 100 µg/mL concentration and Fluconazole was used as reference standard drug.

Minimum inhibition concentration (MIC)

The minimum concentration required for killing all the microorganisms was determined using agar plat method. Standard bacterial strains of *Staphylococcus aureus* (MTCC 3160); *Escherichia coli* and a fungi *Candida albicans* (MTCC 7253) were used in the MIC procedure. The synthetic compounds were dissolved in DMSO at a concentration of 10 mg/ml and for stock

solution. From this stock, 100 µL of sample was serially diluted (500, 250, 125, 62.5 and 31.25 µg/mL) and added in a 96 well petriplate and MIC was determined. Each well containing different concentration of sample (50 µL), 50 µL of diluted microbial cultures and 100 µL of nutrient broth incubated at 37 °C for four h. The antibacterial standard Ciprofloxacin and antifungal standard Fluconazole were also used for comparison. Three microlitres of sample and microbial culture mixture from each well was transferred on nutrient agar plate using a micropipette and checked for any microbial colony growth in the plates after 4 h of incubation at 37 °C. The minimum concentration of the sample which shows complete disappearance of the microbial colony in the plates considered as MIC value of that synthetic compound.

***In vitro* antitubercular activity**

The *in vitro* antimycobacterial activity was performed by Microplate Almer Blue Assay (MABA) method. In this method, due to the metabolic activity of cells, the colour of the Almar blue changes from non-fluorescent blue to a reduced, highly fluorescent pink colour. Middlebrook 7H9 broth base along with Middlebrook OADC growth supplement used as a medium. 100 µL of the Middlebrook 7H9 broth was added to the 96 well plate. 10 mg of drug sample was dissolved in 10 mL of DMSO separately. A stock solution was prepared by diluting 1 mL of the above solution in 9 mL of deionised water and labelled as 100 µg/mL solution. Serial dilutions of 0.8 µg/mL, 1.6 µg/mL, 3.12 µg/mL, 6.25 µg/mL, 12.5 µg/mL, 25 µg/mL, 50 µg/mL and 100 µg/mL were made by diluting the stock solution with deionised water. A positive control was prepared by inoculating the test organism with medium containing standard drugs and a negative control was prepared by inoculating test organism with medium containing only DMSO. The plates were incubated at 37 ^{o}C for five days. After this, 25 µl of freshly prepared 1:1 mixture of Alamar Blue reagent and 10 % Tween 80 was added to the plate and incubated for 24 h. A blue colour in the well was interpreted as no bacterial growth, and pink colour was scored as growth. The MIC was defined as the lowest drug concentration which prohibited the colour change from blue to pink.

Hemolytic assay

The preliminary toxicity of selected potent compounds was tested by hemolytic assay on Red Blood Cells. Human blood was collected in EDTA (2 mg/mL) containing vacutainer. The buffy coat (contains white blood cells and platelets) and plasma were removed from the EDTA-blood. The erythrocytes (RBC) were washed with 0.9 % saline and resuspended in saline to 5 %

suspension. The cells were incubated for 1 h at 37 °C with test compounds of 4 different concentrations (12.5, 25, 50 and 100 µg/mL). The samples were centrifuged after incubation and the absorbance was recorded by using a UV spectrophotometer. Triton X-100 (2%, Sigma-Aldrich, St. Louis, USA) and phosphate buffered saline were used as positive and negative control respectively. The absorbance of haemoglobin release was measured at 540 nm and is expressed as % of Triton X- 100 induced hemolysis. The result was calculated by using the formula,

% Hemolysis = [(Absorbance of the sample) – (Absorbance of blank)/ Highest absorbance of positive control] x 100.

Each concentration had triplicate values. HC_{50} was determined for each triplicate OD and an average of HC_{50} was plotted against concentration fitted with a sigmoid plot. From the curve concentration corresponding to 50% hemolysis was determined.

Molecular Docking

To test the docking parameters low energy conformations of all compounds were docked into the catalytic pocket of the receptor protein AK (PDB-ID: 4ZTR) using Grid-Based Ligand Docking With Energetics (Glide v7.8, Schrödinger 2018-1)[1] in 'extra precision' mode without applying any constraints. The final best docked structure was selected using a Glide score function, Glide energy and Glide Emodel energy. Finally, the lowest-energy docked complex of **6i**/4ZTR and **7e**/4ZTR were selected for further study. As other molecules interaction with hinge region of catalytic pocket was not satisfactory, Compounds **6i** and **7e** were subjected for Induced fit docking.

Induced fit docking

Schrodinger's Induced Fit Docking (IFD) module was used for docking analyses of the two compounds with best interaction *i.e.* **6i** and **7e**. LigPrep module was used to prepare the ligands and was submitted as starting geometries to IFD. The IFD has the ability of sampling the minor changes in the backbone structure as well as robust conformation changes in side chains. A softened-potential docking is performed in the first IFD stage where docking of the ligand occurs into an ensemble of the binding protein conformations. Subsequently, complex minimization for highest ranked pose is performed where both the ligand and binding sites are free to move.

MD Simulation

The experimental was same for both **6i**/4ZTR and **7e**/4ZTR complexes. The molecular system was solvated with water molecules in an orthorhombic box (volume 4ZTR⁄1563074 $Å^3$) allowing for a 10 Å buffer region between protein atoms and box sides. The total numbers of atoms in solvated protein structure for the MD simulations are more than 37,760 (including 33,408 water molecules) whereas the total number of atoms of 4ZTR with the substrate was approximately 4304. The system was placed at a distance of 10 Å from the edge of the box and LBFGS minimization was performed with 3 vectors and minimum 10 steepest descent steps until a gradient threshold of 25 kcal/mol/Å was reached. The maximum iterations during minimization were 2000 and convergence threshold was kept at 1.0 kcal/mol/Å. For long range electrostatic interactions Smooth Particle Mesh Ewald[2] method was used at a tolerance of 1e # 09 and a cut-off radius of 9 Å was selected for short range electrostatic interactions. Before equilibration and MD simulations, the system was minimized and pre-equilibrated using the default relaxation routine implemented in Desmond. Then the system was gradually heated in the NPT ensemble to 300° K with a time step of 2 fs. A 10 ns MD simulation in the NPT ensemble (T1⁄4 300 °K, thermostat relaxation time 1⁄4200 ps; P 1⁄41 atm; barostat relaxation time 1⁄4200 ps) was performed using a Nose–Hoover thermostat[3] and Martyna–Tobias–Klein barostat[4]. Data were collected every 100 ps during MD run. 3D structures and trajectories were visually inspected using the Maestro graphical interface. An average structure obtained from the last 250 ps of MD simulation was refined by means of 1000 steps of steepest descent followed by conjugate gradient energy minimization. The maximum number of cycle of minimization was 5000 and the convergence criterion for the energy gradient was 0.001 kJ/mol/Å.

Target Identification

In efforts to understand the significant difference between cytotoxicity of thiazolidinone derivatives in MDA-MB-231 cell line and HepG2 Cell lines it found necessary to identify the mechanism of action of compounds. In that regard the cell biology of both breast cells and hepatocytes was studied. During then, it was understood that, there are different signaling pathways involved in the differentiation of normal breast cell and liver cell into cancer cells. The protein expression data provided in Genecards database also supported the same and proposed a signaling pathway called Aurora kinase pathway is enabled in only MDA-MB-231 cell line but

not in HepG2 cell lines. Further, it is understood that, Aurora-2 is a key member of a closely related subgroup of serine/threonine kinases that plays important roles in the completion of essential mitotic events in breast cells. Aurora-2 is oncogenic and amplified in various human cancers and could be an important therapeutic target for inhibitory molecules that would disrupt the cell cycle and block proliferation. The binding modes of Aurora kinase inhibitors to Aurora kinases share specific hydrogen bonds between the inhibitor core and the back bone of the kinase hinge region, while others parts of the molecules may point to different parts of the active site via non-covalent interactions. Currently there are about 30 Aurora kinase inhibitors in different stages of pre-clinical and clinical development. Hence, in the current study Aurora kinase was identified as potent target and subjected for computational modeling studies.

The Aurora kinase structure 6,12,16,17 represents a typical bilobal kinase fold containing the N-terminal -strand domain and the C-terminal R-helix domain. The two domains are linked by a hinge region (residues 210-216), a loop forming the conserved hydrogen bonding interactions with the ATP or inhibitors, which is sandwiched between the two domains. The conserved H-bonding interactions of inhibitors with hinge region residues Glu211 and Ala213 are observed in most of the inhibitor-Aurora complex structures and are essential for maintaining activity. Meanwhile, classical AK inhibitors target the conserved ATP site in the DFG(Asp-Phe-Gly)-in conformation or explore the allosteric site exposed through the classic DFG-flip[5,6]. However, there are some inhibitors which target an unusual non DFG-out conformation called DFG-out (up) conformation which is formed through ligand-induced conformational changes and results in switching the character of the active site from polar to hydrophobic. This conformation is formed when the DFG-loop is ushered to a location parallel to the αC-helix unlike the regular DFG-out wherein it swaps out of the active site. With all these considerations, multiple docking poses were generated when 15 thiazolidinone derivatives and co-crystal 4RJ were subjected to docking simulation by successful execution of IFD against the catalytic pocket of the receptor protein AK. The best poses for **6i** and **7e** were utilized for further computational analyses. Similarly, the best pose of the bound native ligand, 4RJ was used for analyses after the IFD.

ESI references

1. R. A. Friesner, R. B. Murphy, M. P. Repasky, L. L. Frye, J. R. Greenwood, T. A. Halgren, P. C. Sanschagrin and D. T. Mainz, *J. Med Chem*. 2006, **49**, 6177.

2. U. Essmann, L. Perera and M. L. Berkowitz, *J. Chem. Phys*., 1995, **103**, 8577.
3. G. J. Martyna and M. L. Klein, *J. Chem. Phys*., 1992, **97**, 2635.
4. G. J. Martyna, *J. Chem. Phys*., 1994, **101**, 4177.
5. Z. Zhao, H. Wu, L. Wang, Y. Liu, S. Knapp, Q. Liu and N. S. Gray, *ACS Chem. Biol*., 2014, **9**, 1230.
6. M. A. Seeliger, P. Ranjitkar, C. Kasap, Y. Shan, D. E. Shaw, N. P. Shah, J.Kuriyan, D. J. Maly, *Cancer Res.*, 2009, **69**, 2384.

Selected spectra of compounds

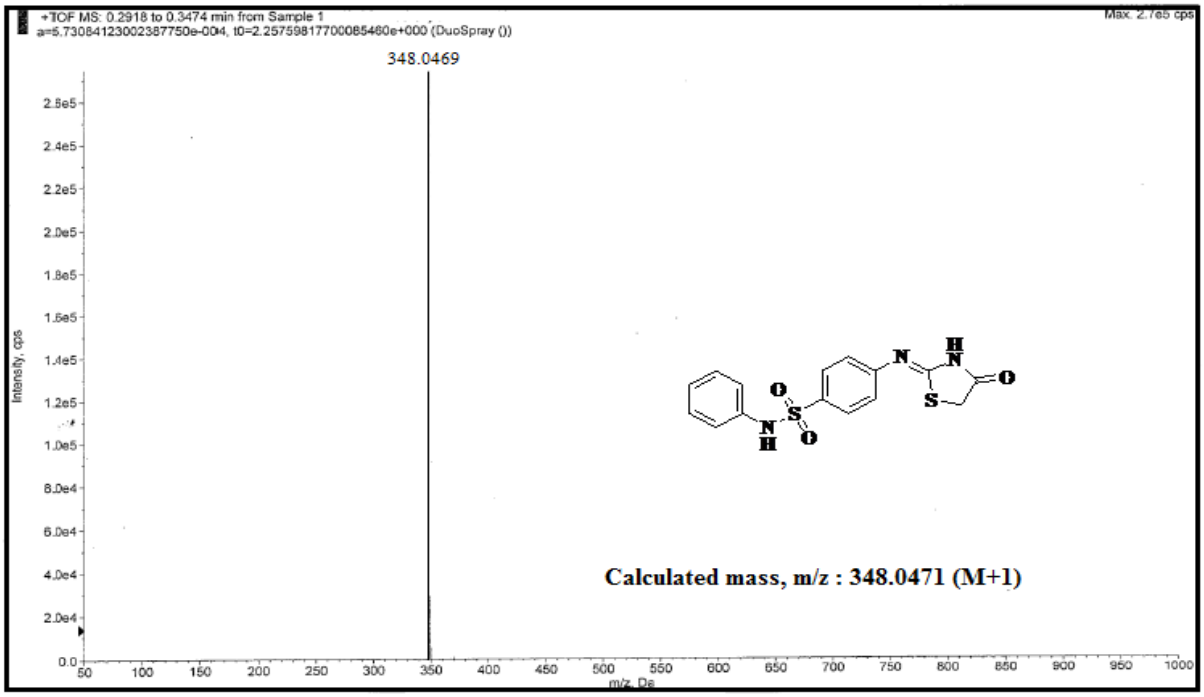

Fig. S1 The HRMS spectrum of compound **5a**.

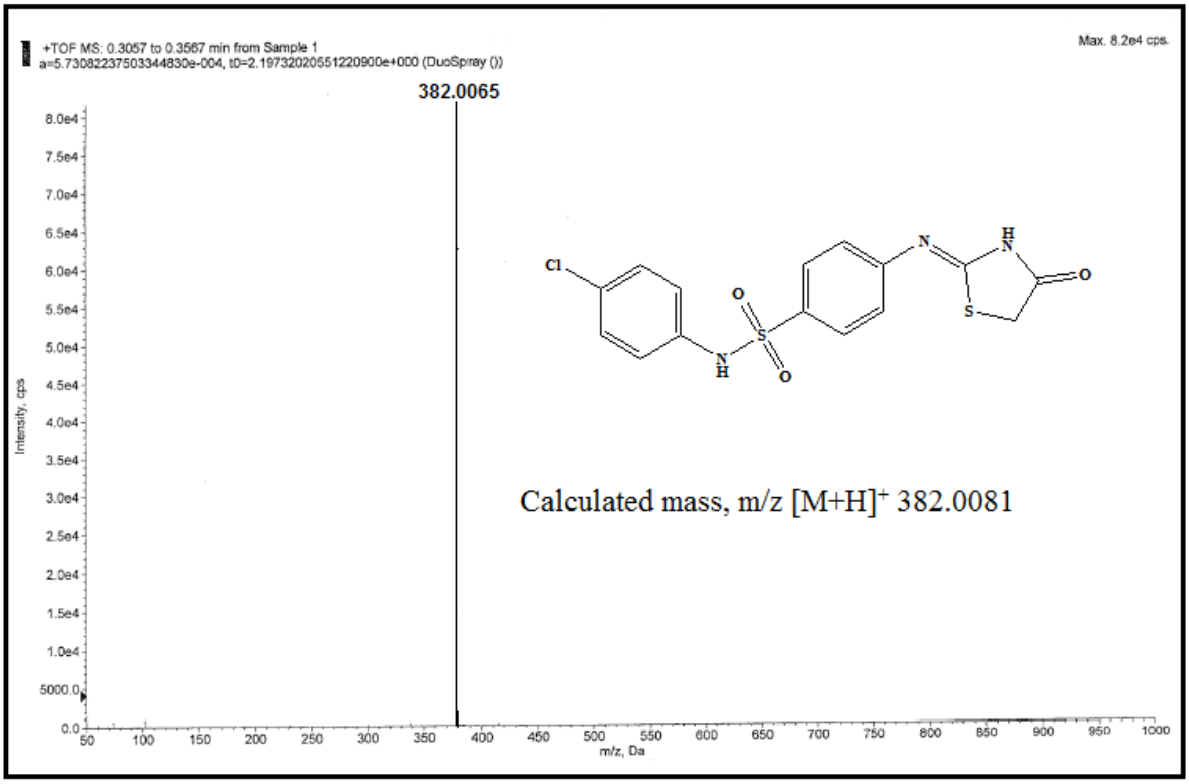

Fig. S2 HRMS spectrum of compound **5b**.

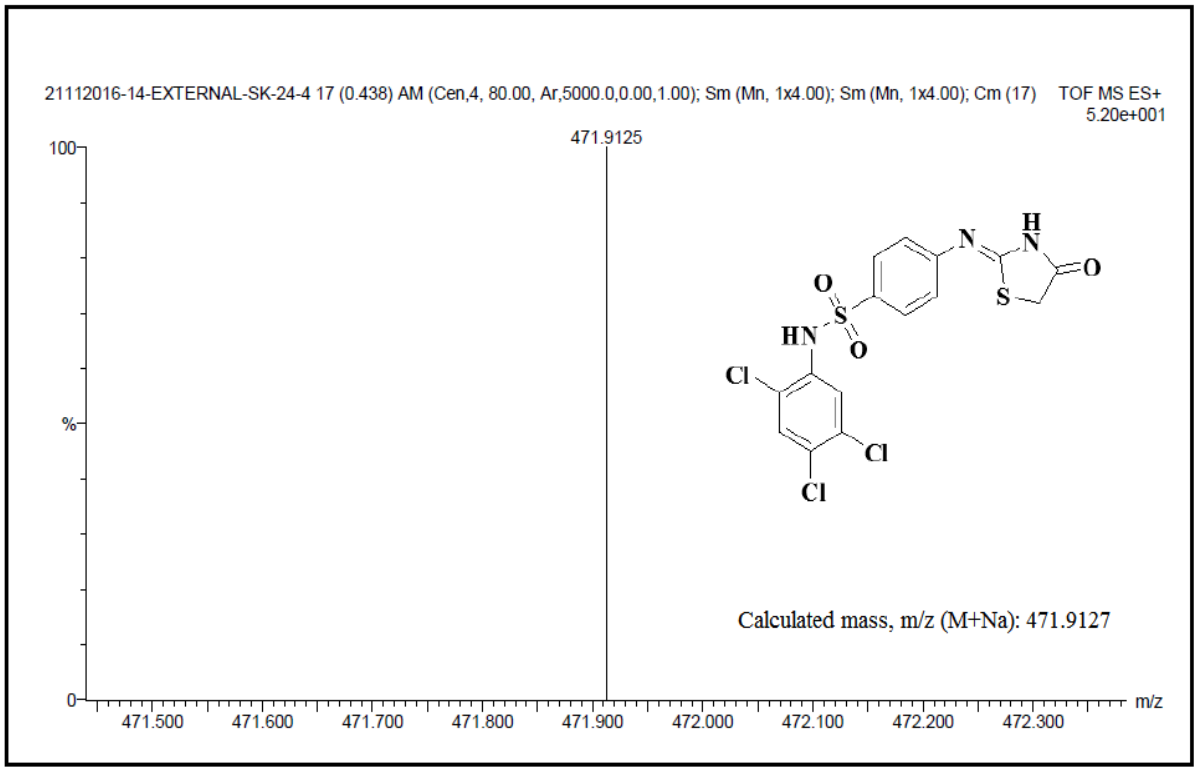

Fig. S3 HRMS spectrum of compound **5i**.

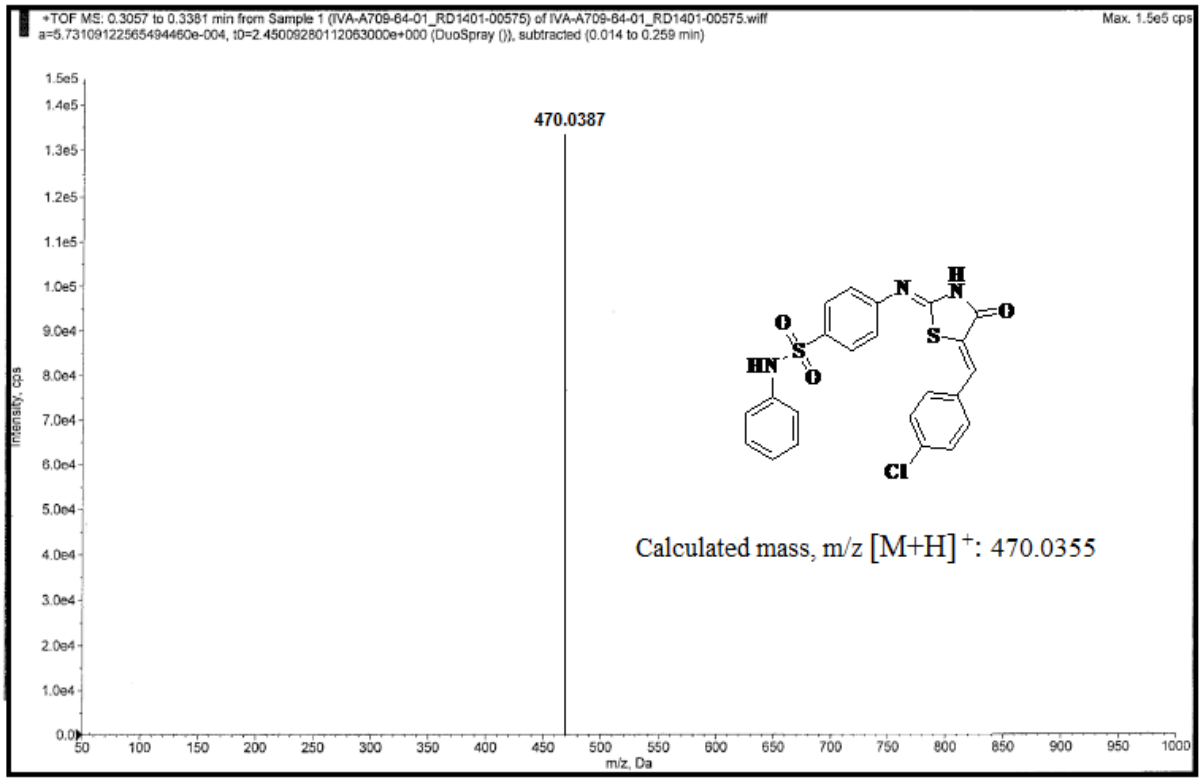

Fig. S4 HRMS spectrum of compound **6a**

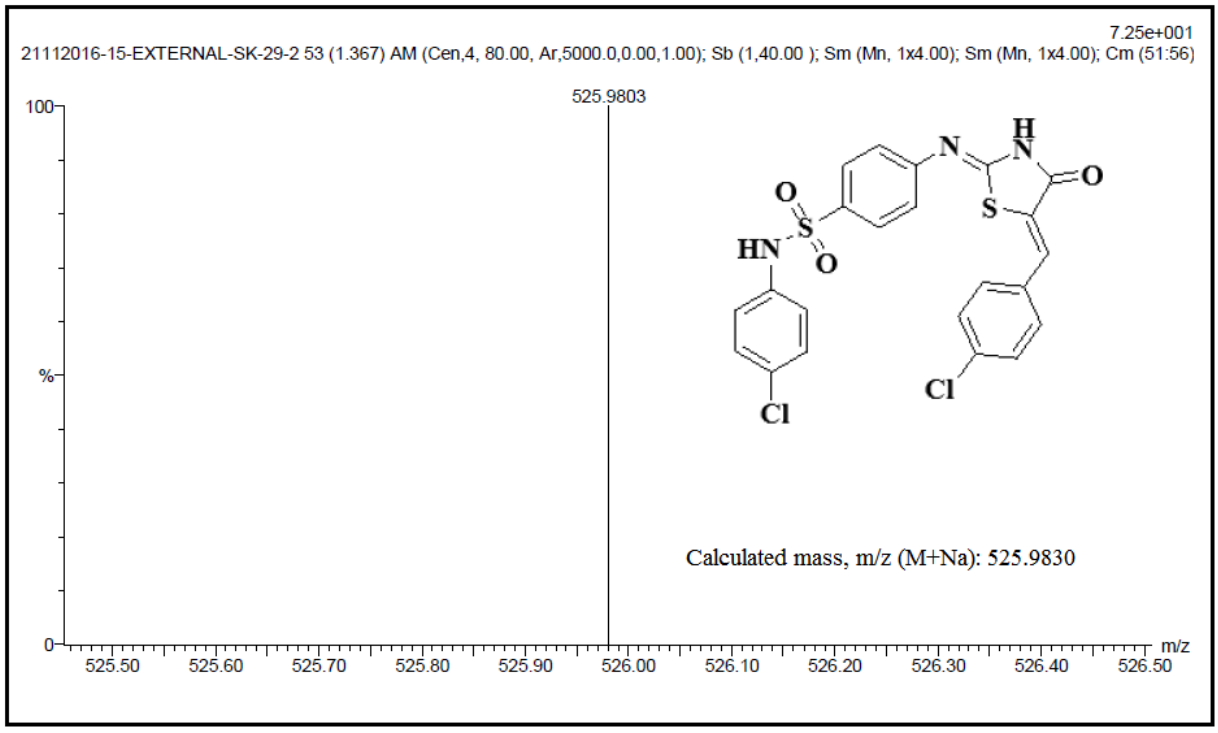

Fig. S5 HRMS spectrum of compound **6d**.

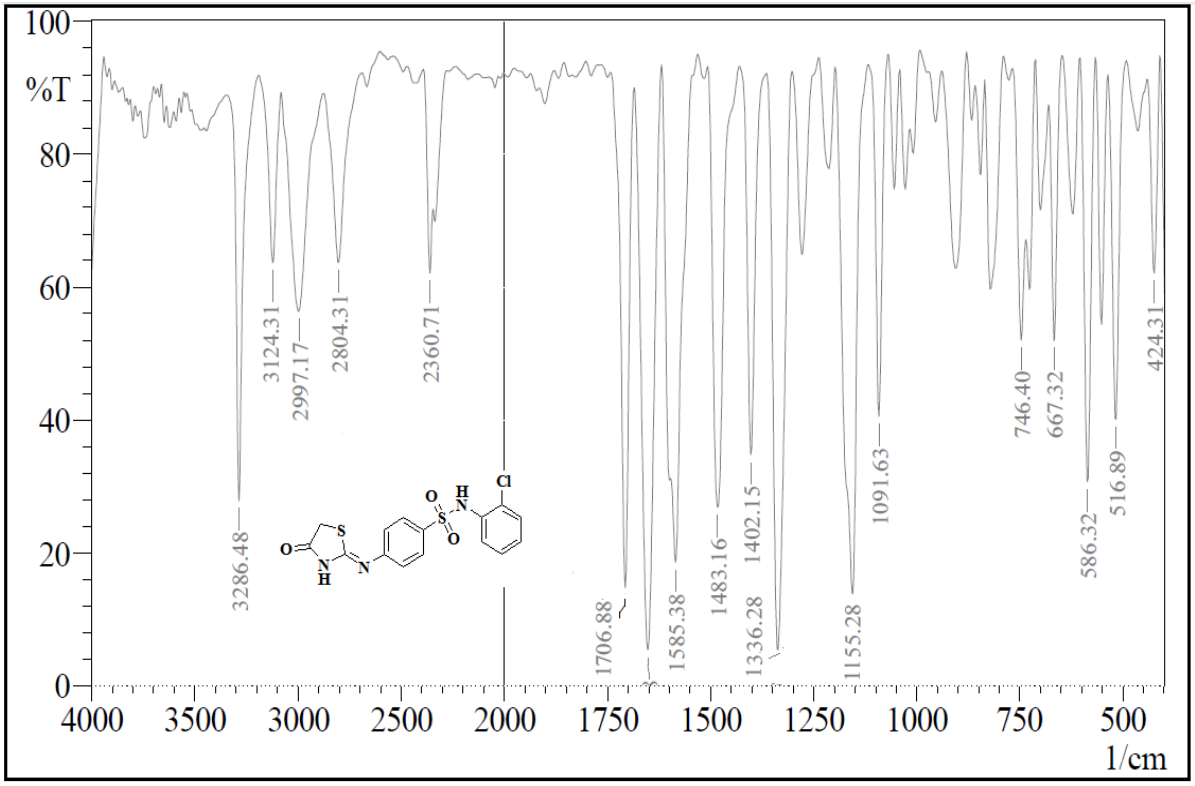

Fig. S6 FT-IR spectrum of compound **5b**.

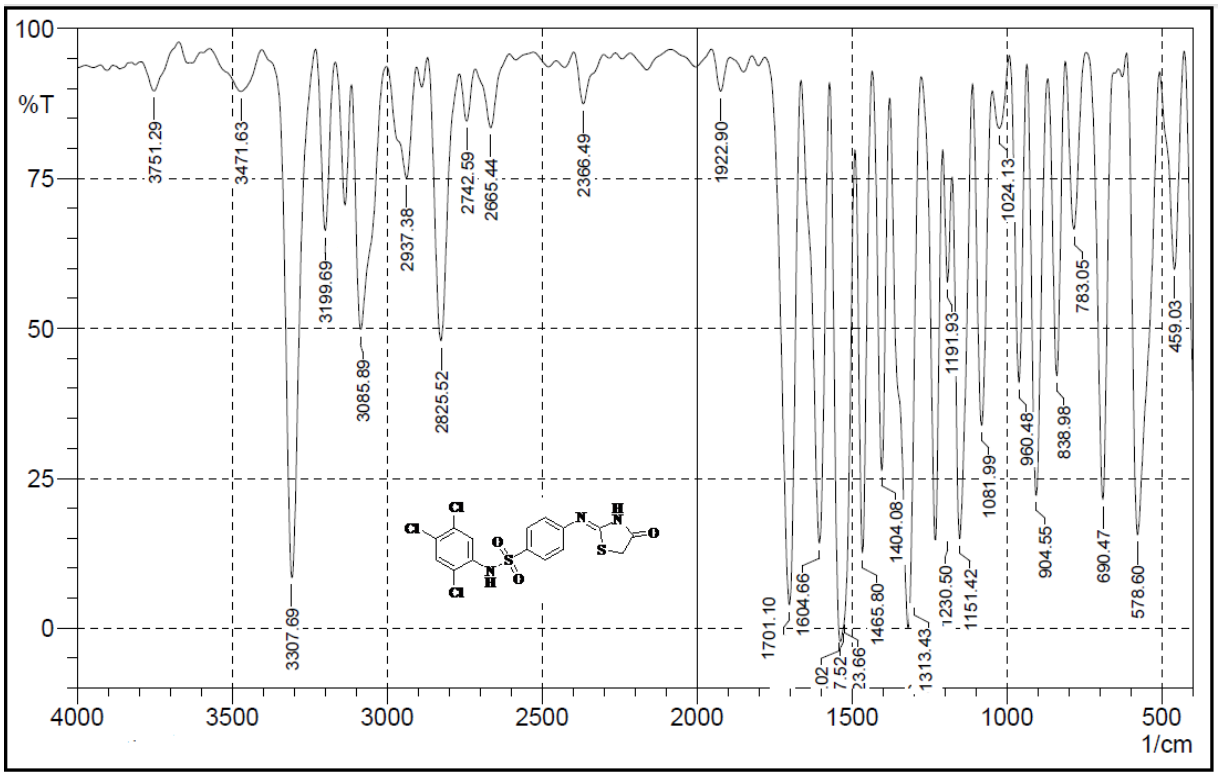

Fig. S7 FT-IR spectrum of compound **5i**.

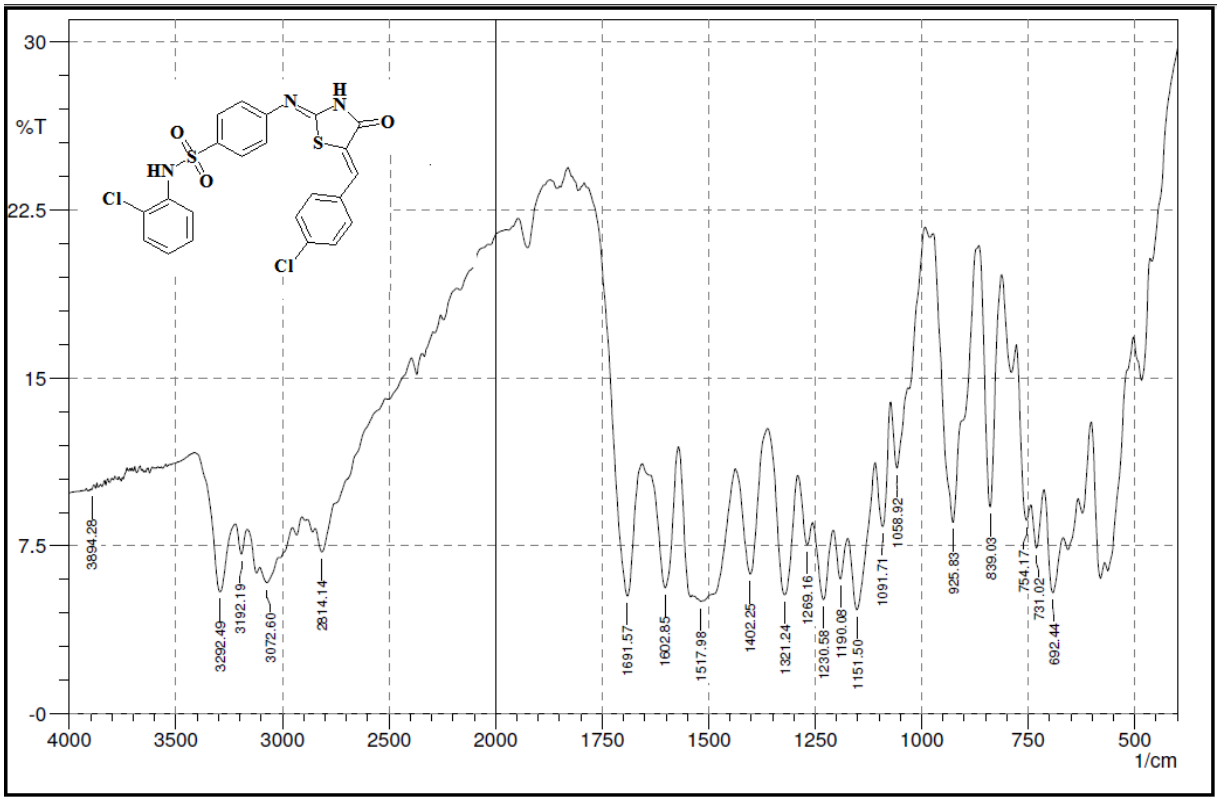

Fig. S8 FT-IR spectrum of compound **6b**.

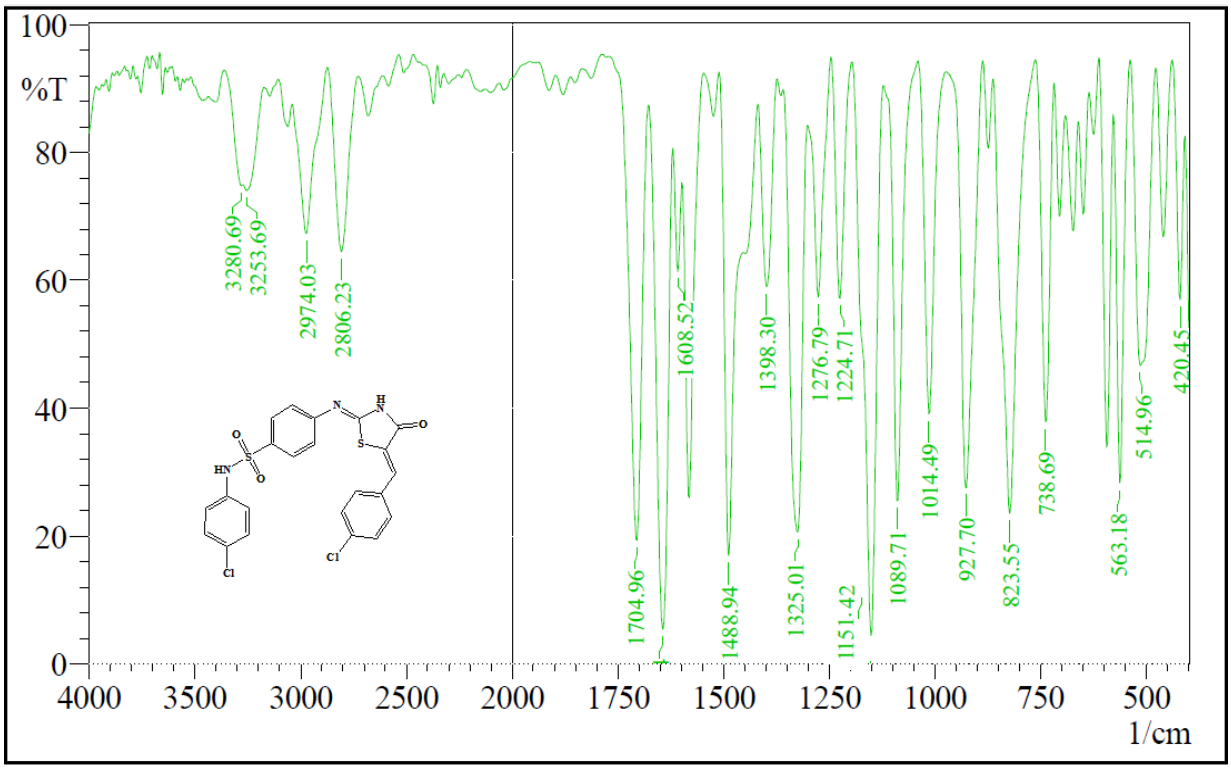

Fig. S9 FT-IR spectrum of compound **6d**.

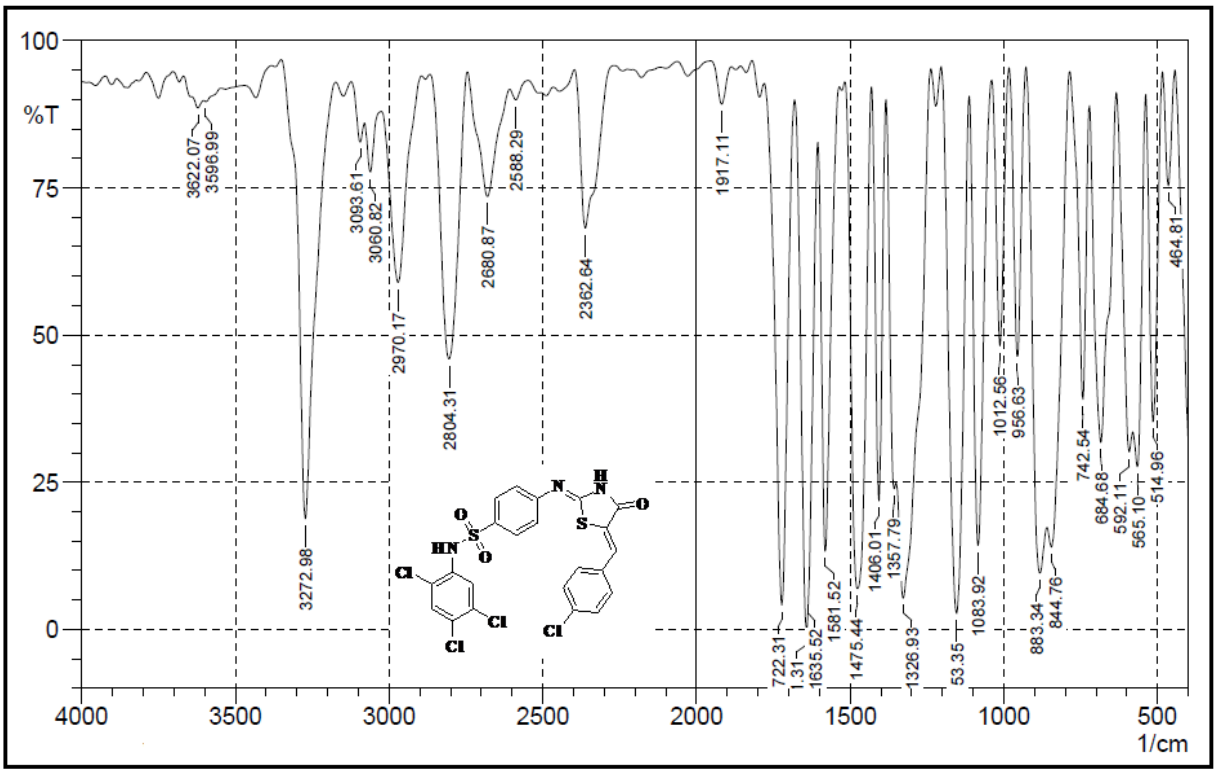

Fig. S10 FT-IR spectrum of compound **6i**.

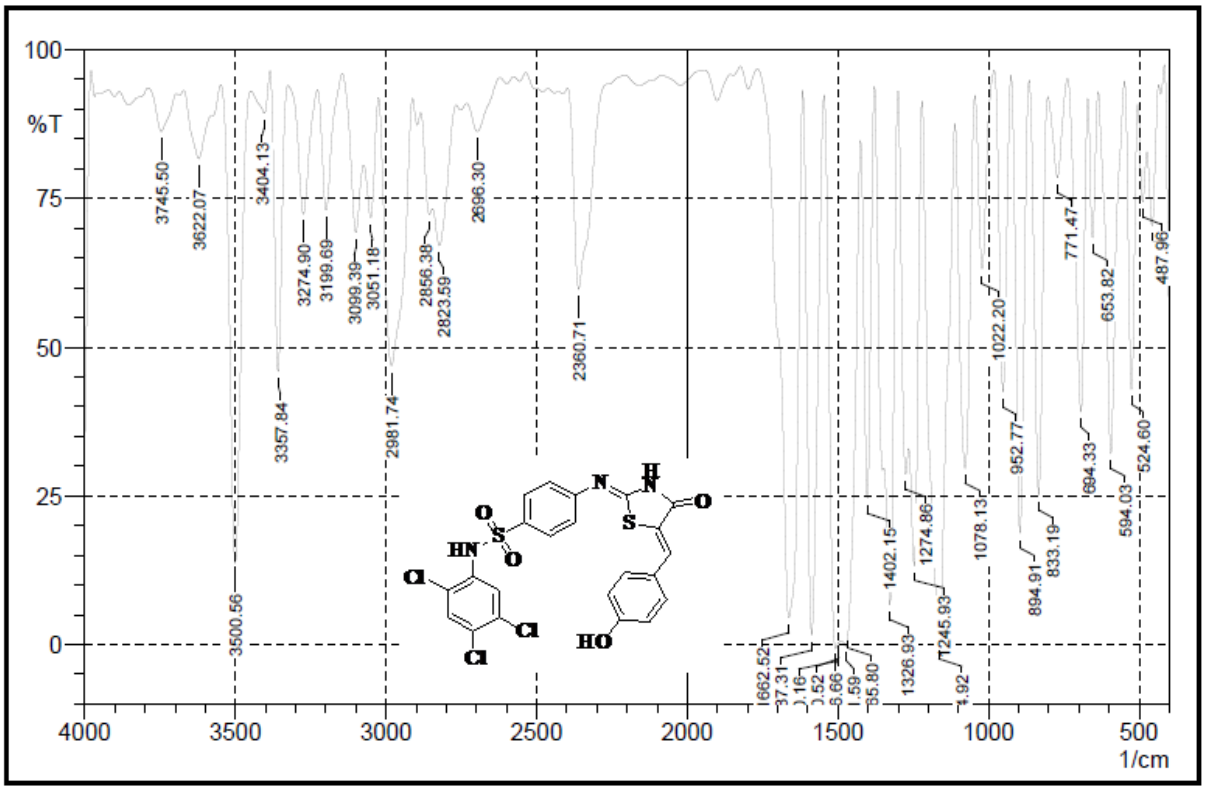

Fig. S11 FT-IR spectrum of compound **7e**.

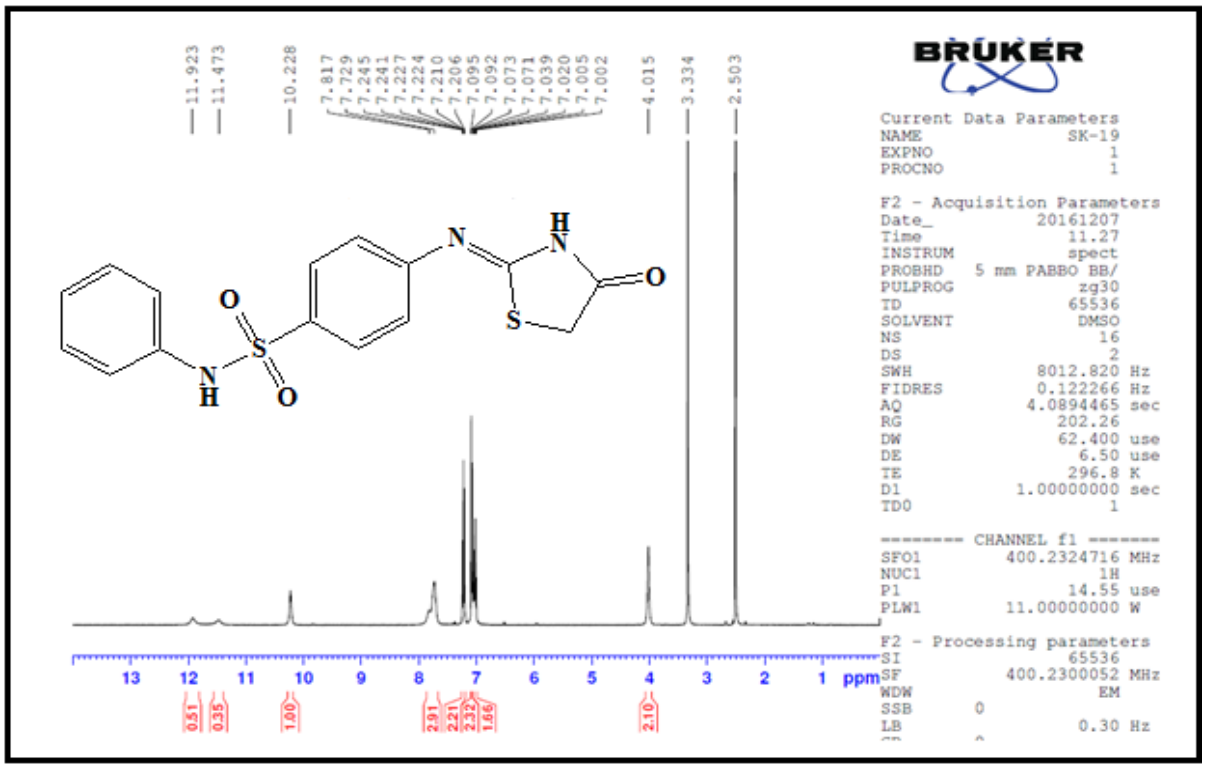

Fig. S12 ^{1}H NMR spectrum of compound **5a**.

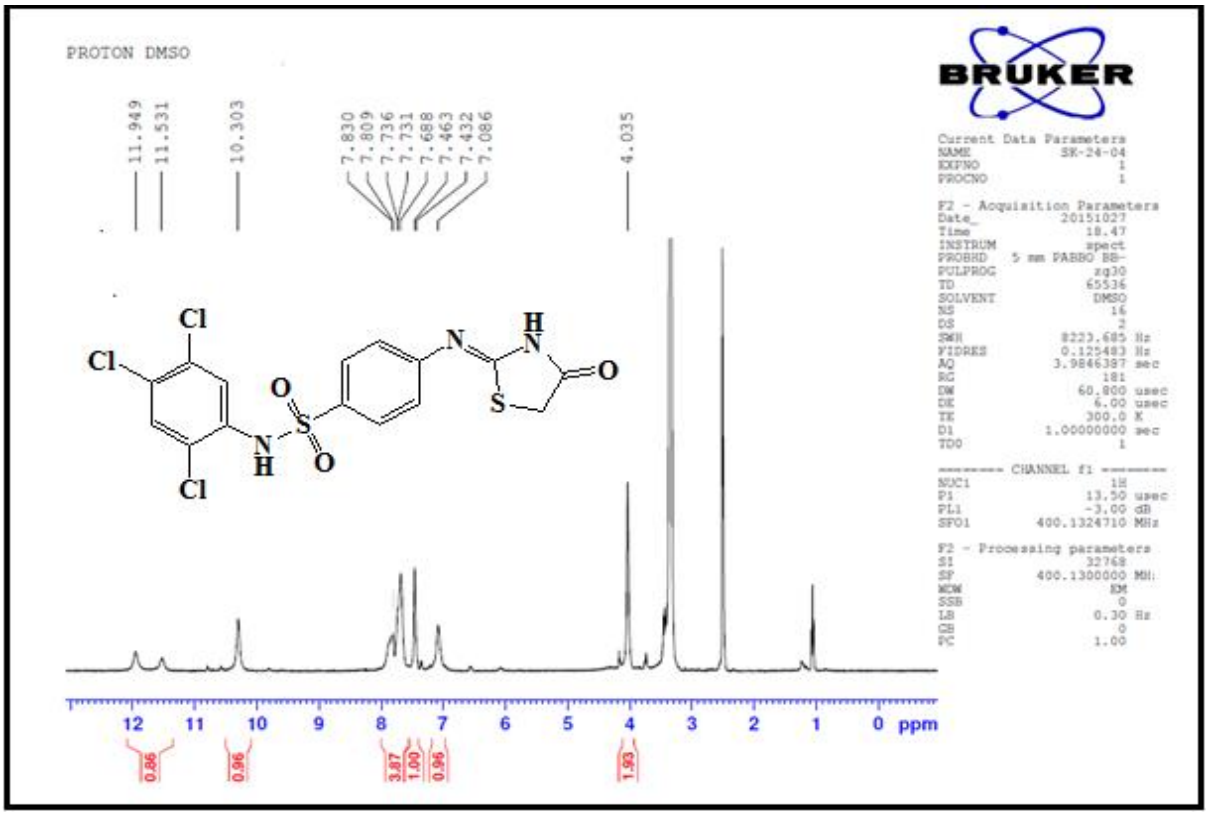

Fig. S13 ^{1}H NMR spectrum of compound **5i**.

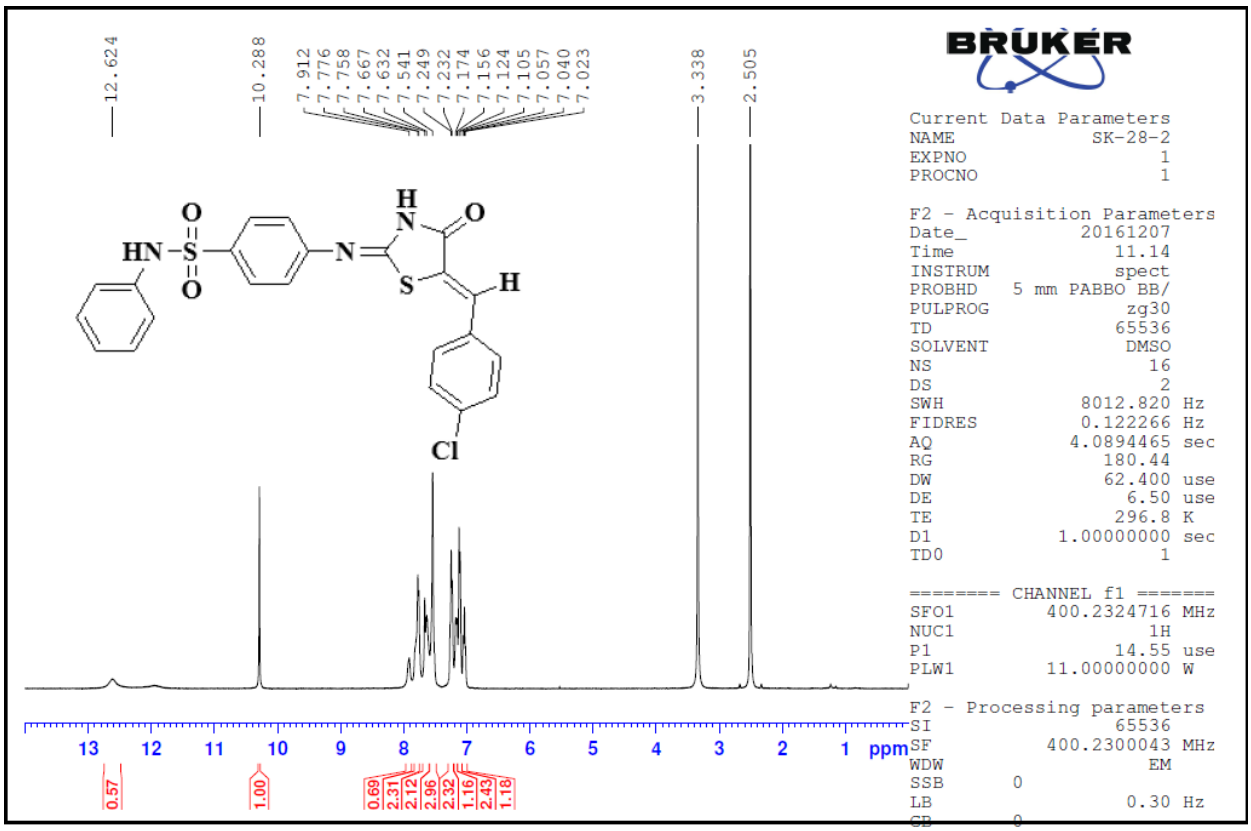

Fig. S14 ^{1}H NMR spectrum of compound **6a**.

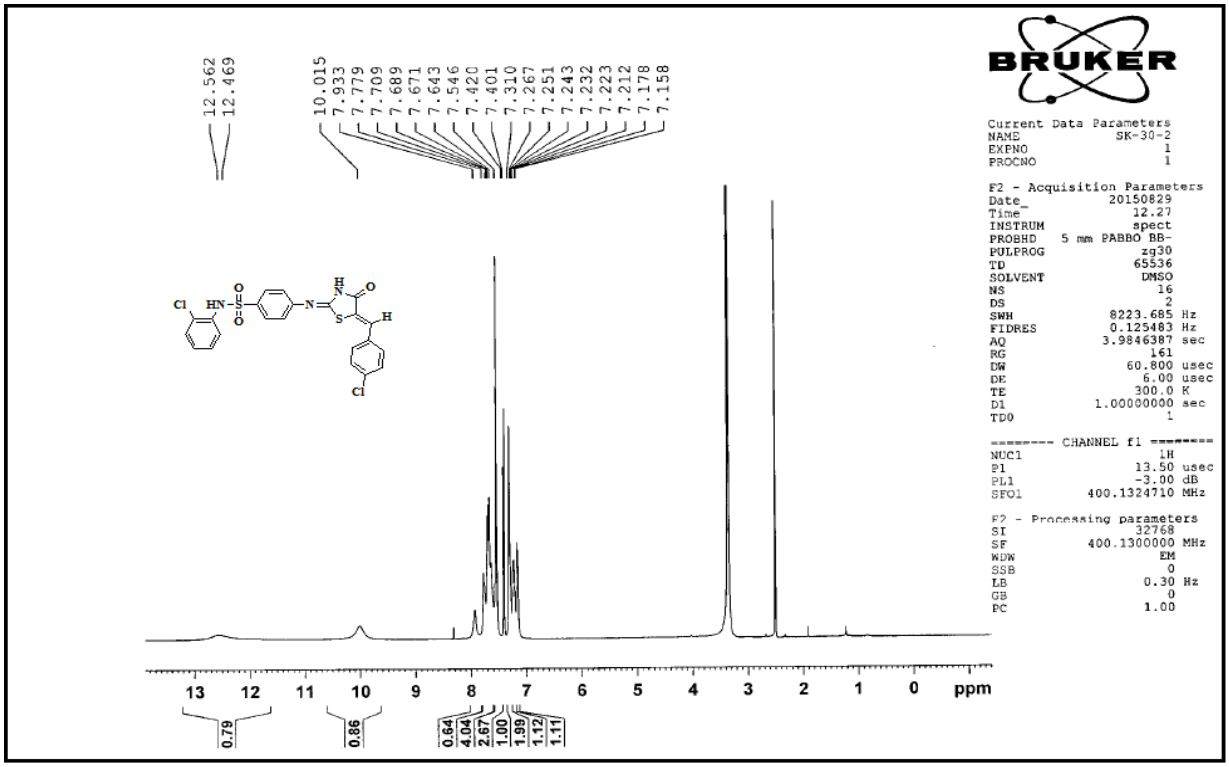

Fig. S15 ^{1}H NMR spectrum of compound **6b**.

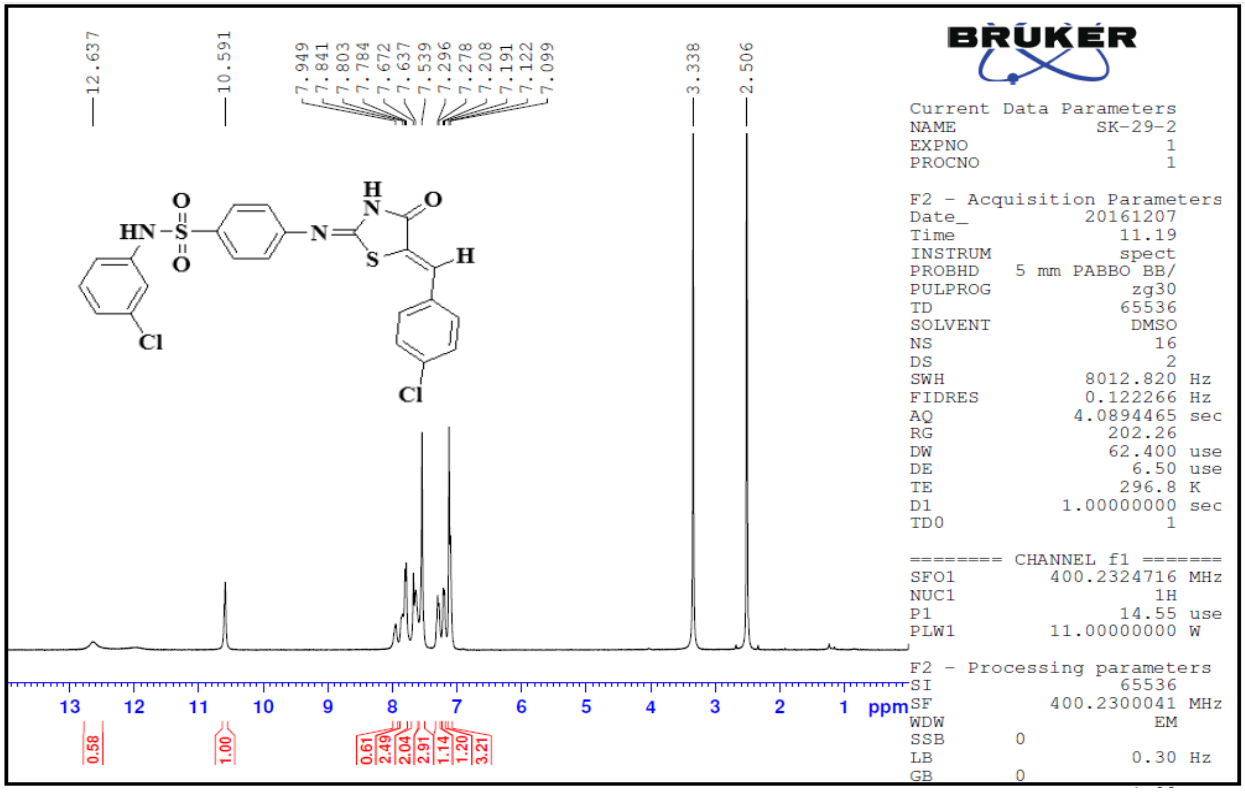

Fig. S16 ^{1}H NMR spectrum of compound **6c**.

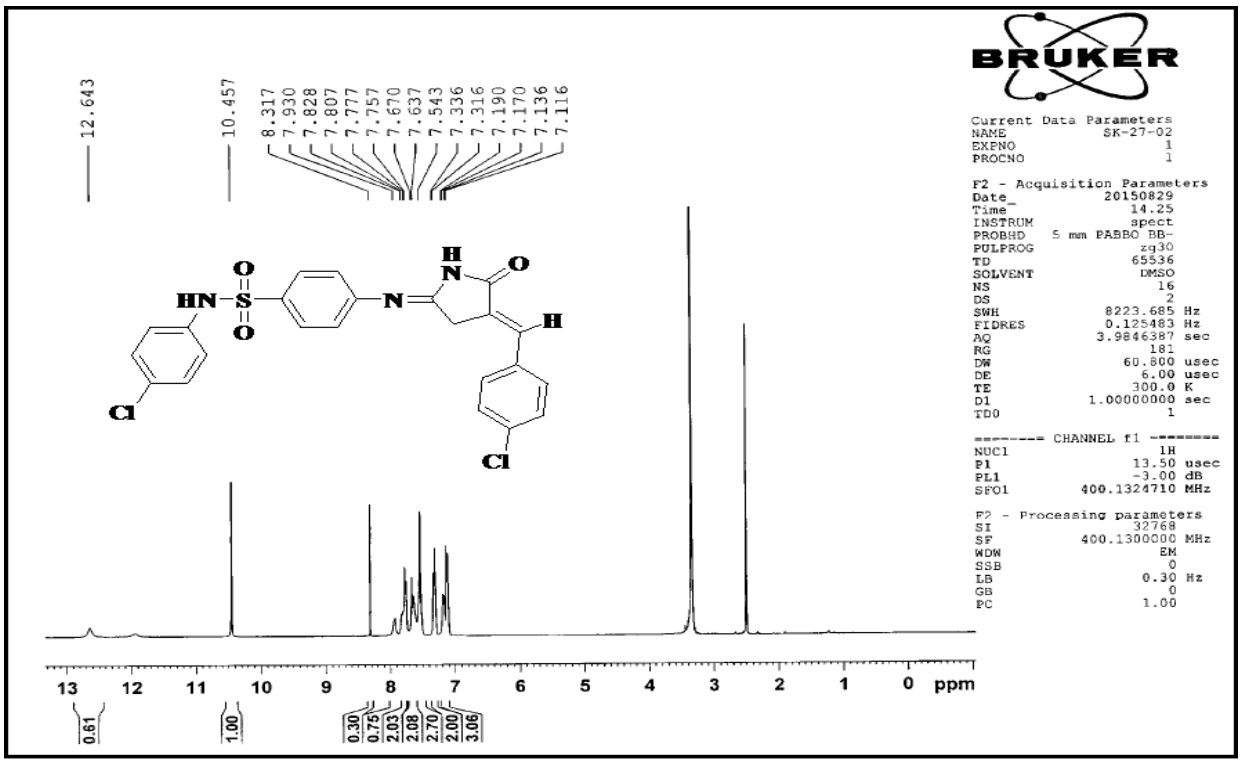

Fig. S17 ^{1}H NMR spectrum of compound **6d**.

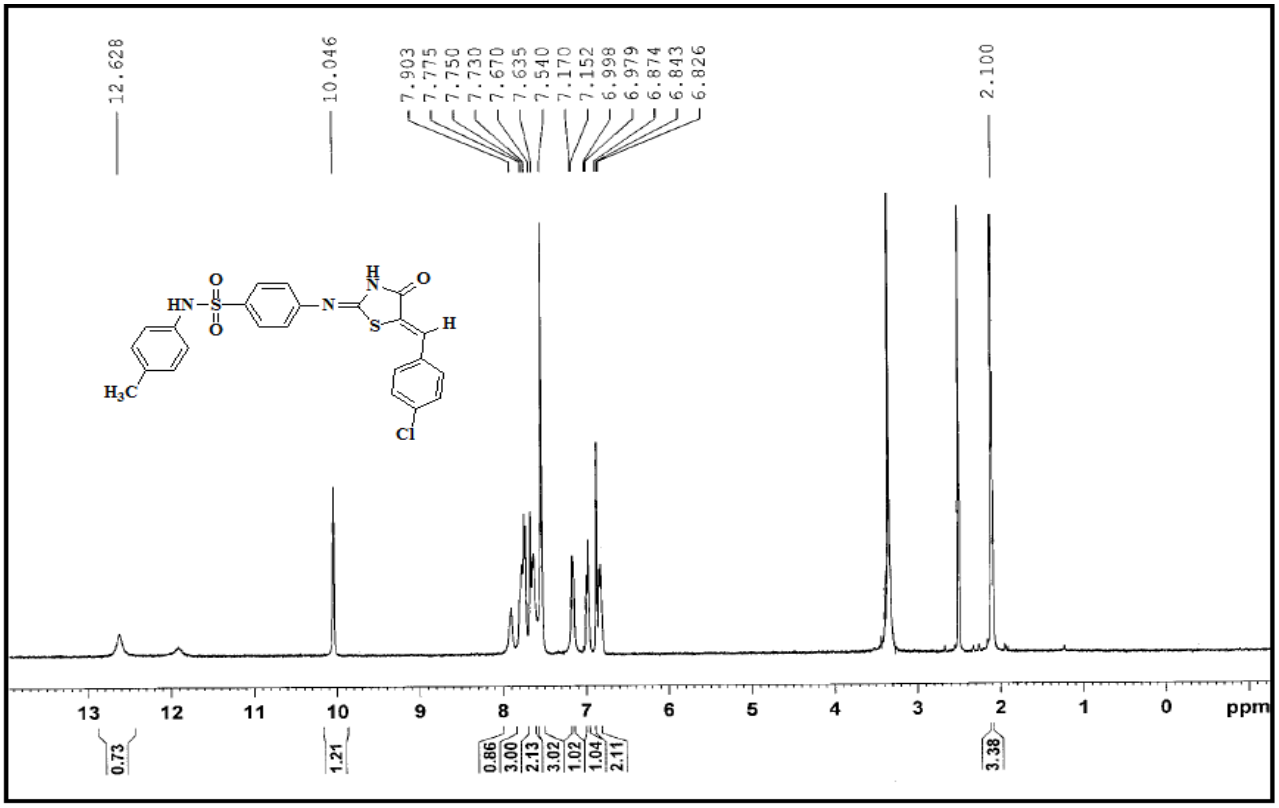

Fig. S18 ^{1}H NMR spectrum of compound **6e**.

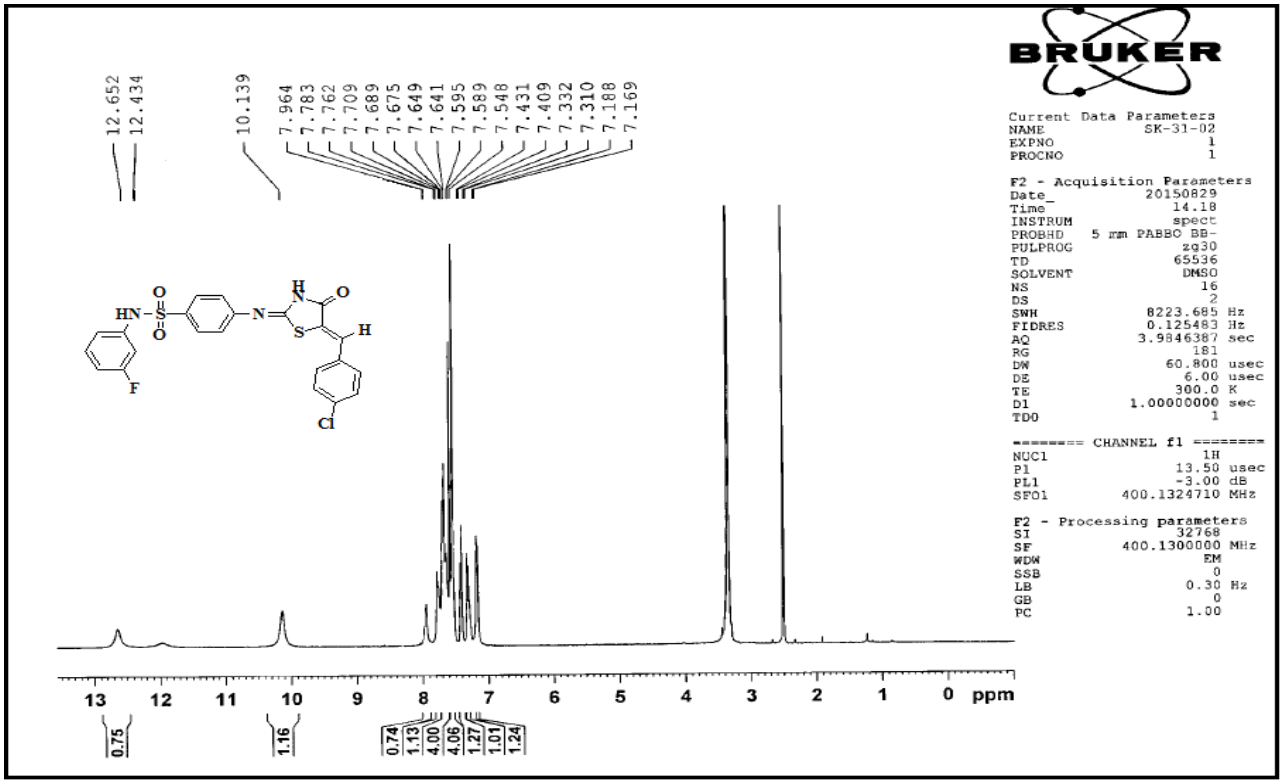

Fig. S19 ^{1}H NMR spectrum of compound **6f**.

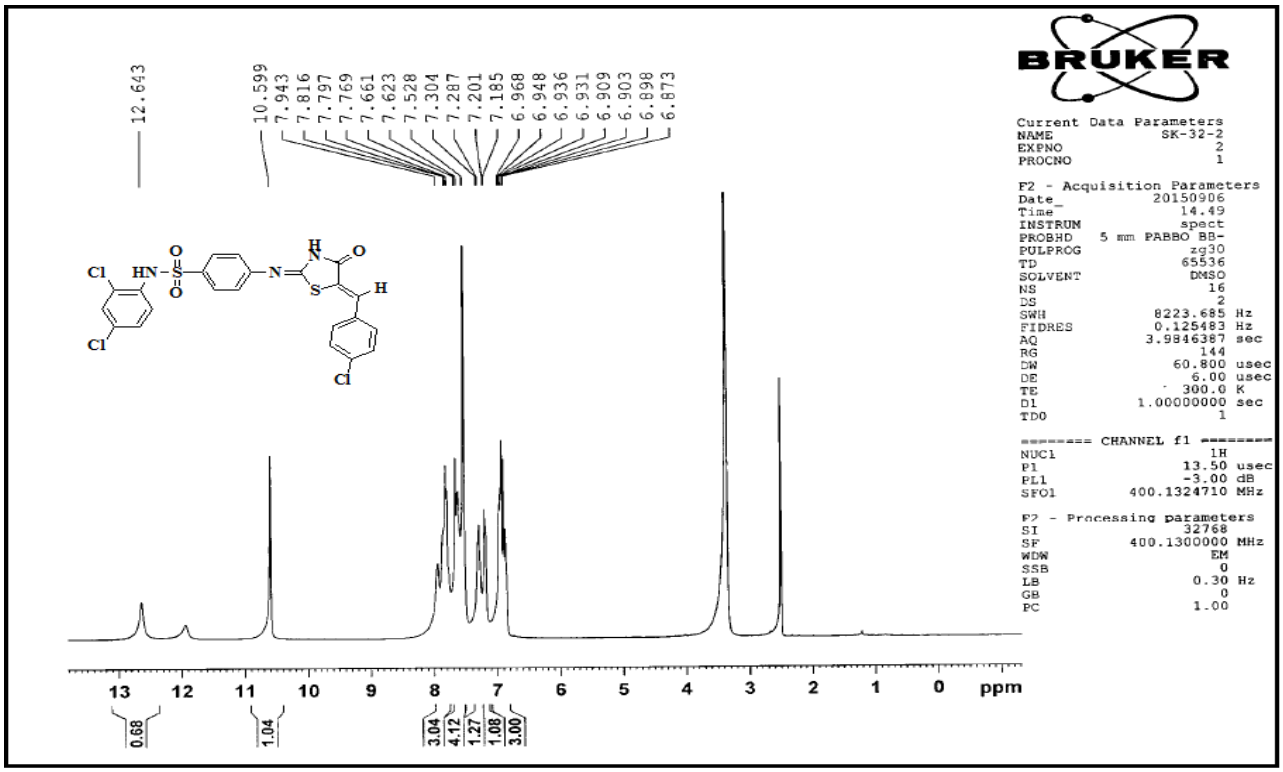

Fig. S20 ^{1}H NMR spectrum of compound **6g**.

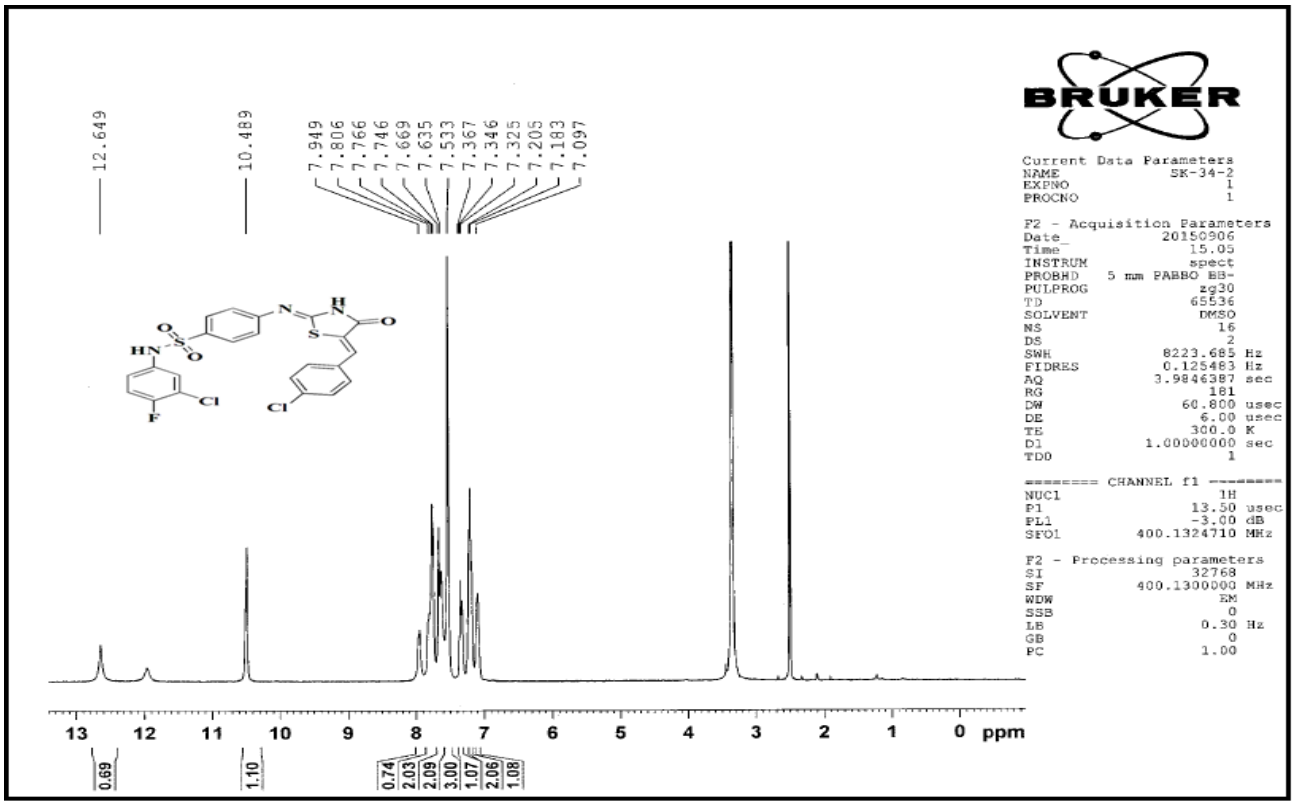

Fig. S21 ^{1}H NMR spectrum of compound **6h**.

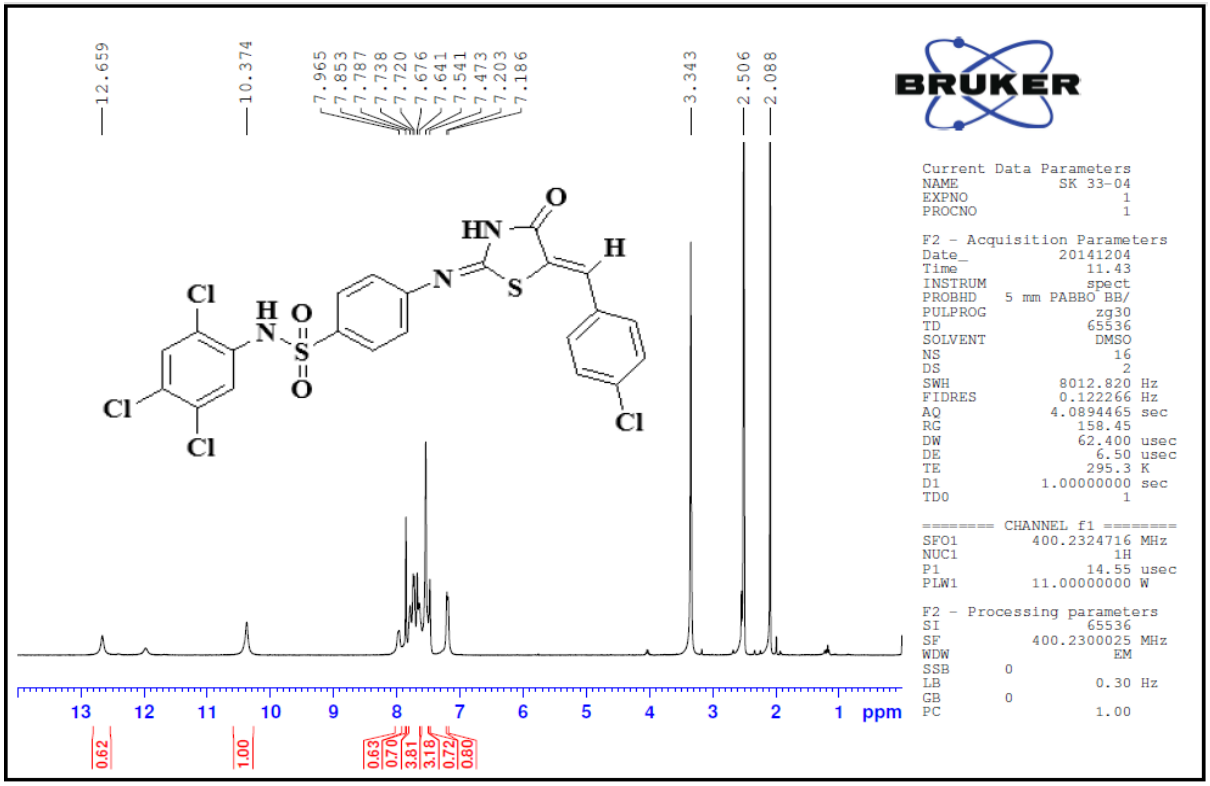

Fig. S22 ^{1}H NMR spectrum of compound **6i**.

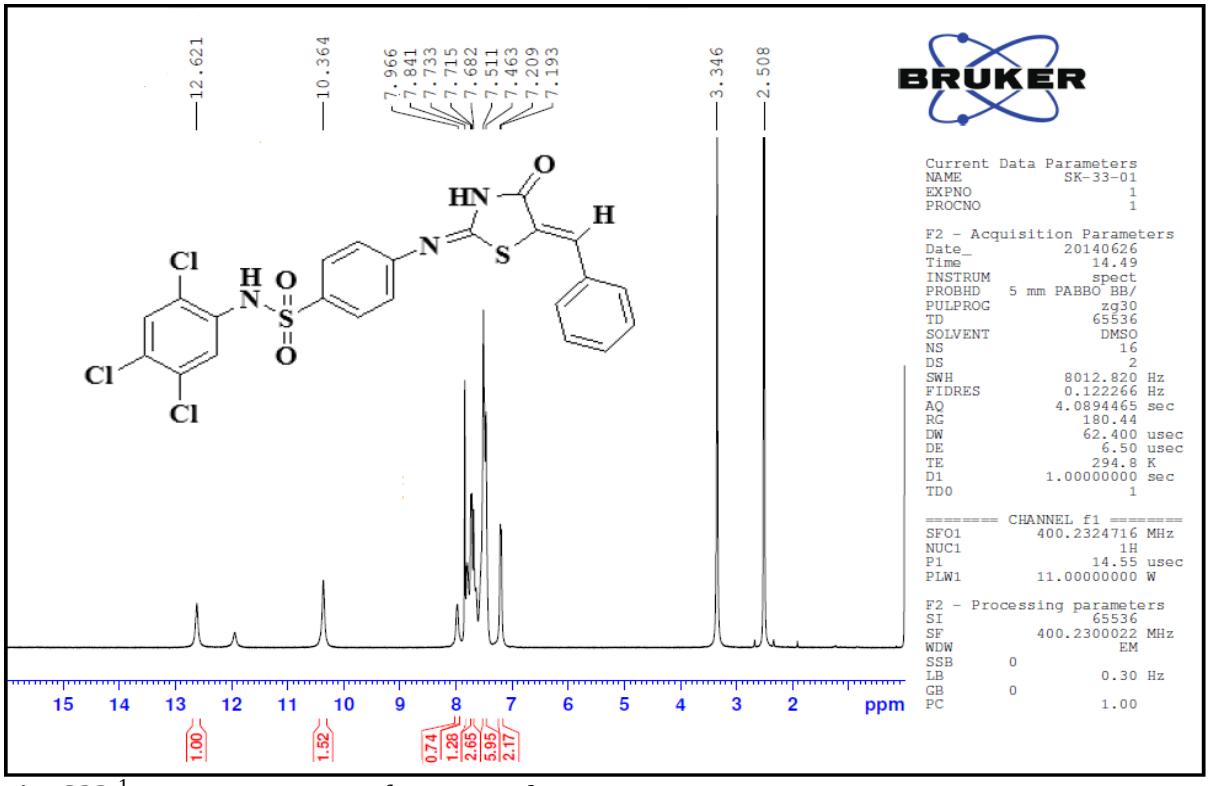

Fig. S23 ^{1}H NMR spectrum of compound **7a**.

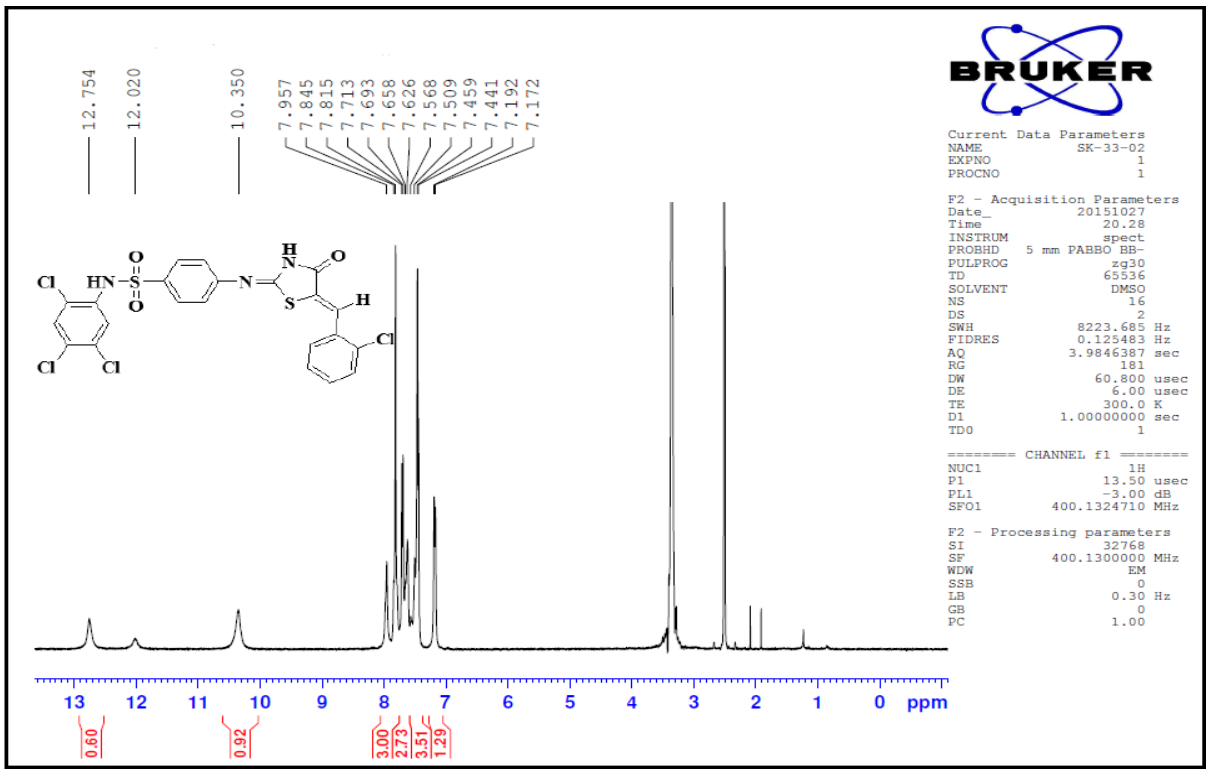

Fig. S24 ^{1}H NMR spectrum of compound **7b**.

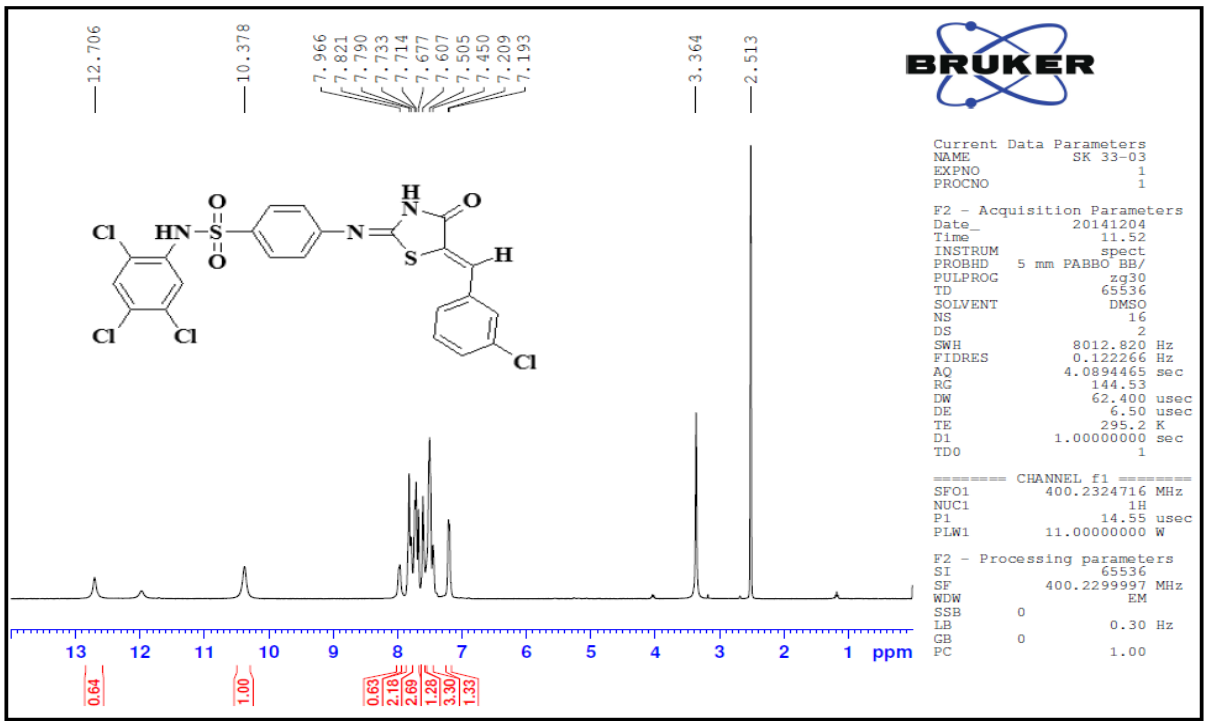

Fig. S25 ^{1}H NMR spectrum of compound **7c**.

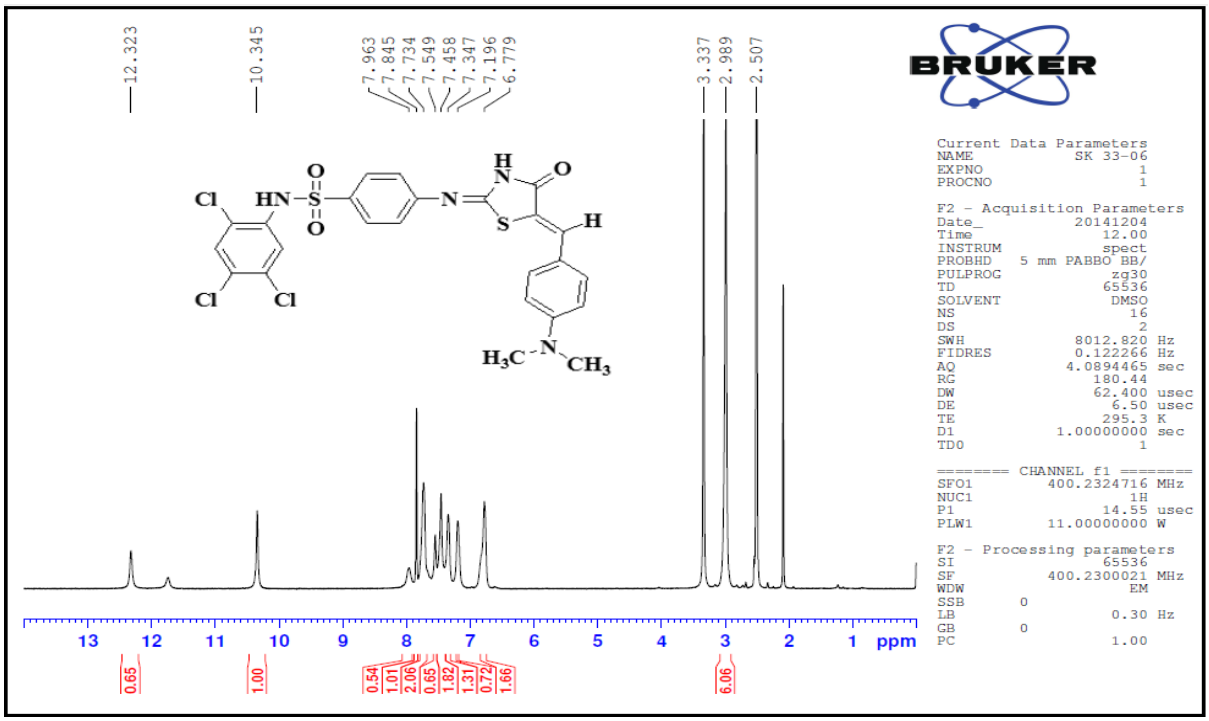

Fig. S26 ^{1}H NMR spectrum of compound **7d**.

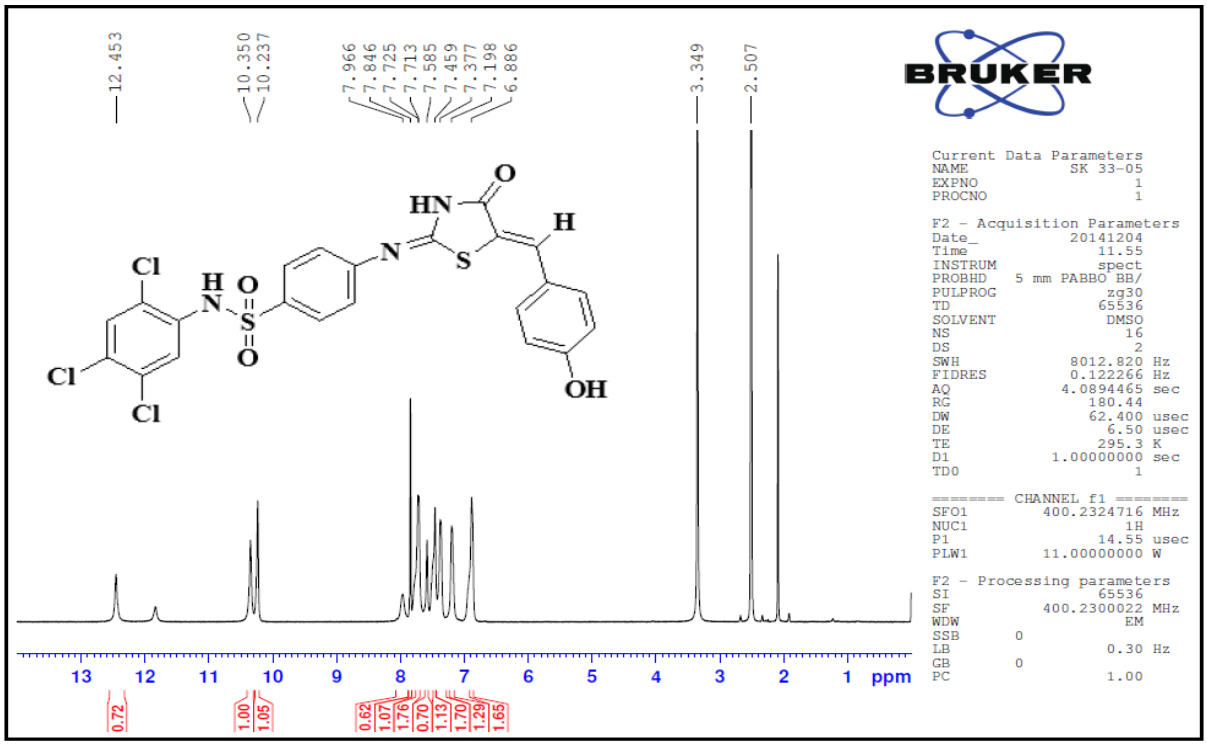

Fig. S27 ^{1}H NMR spectrum of compound **7e**.

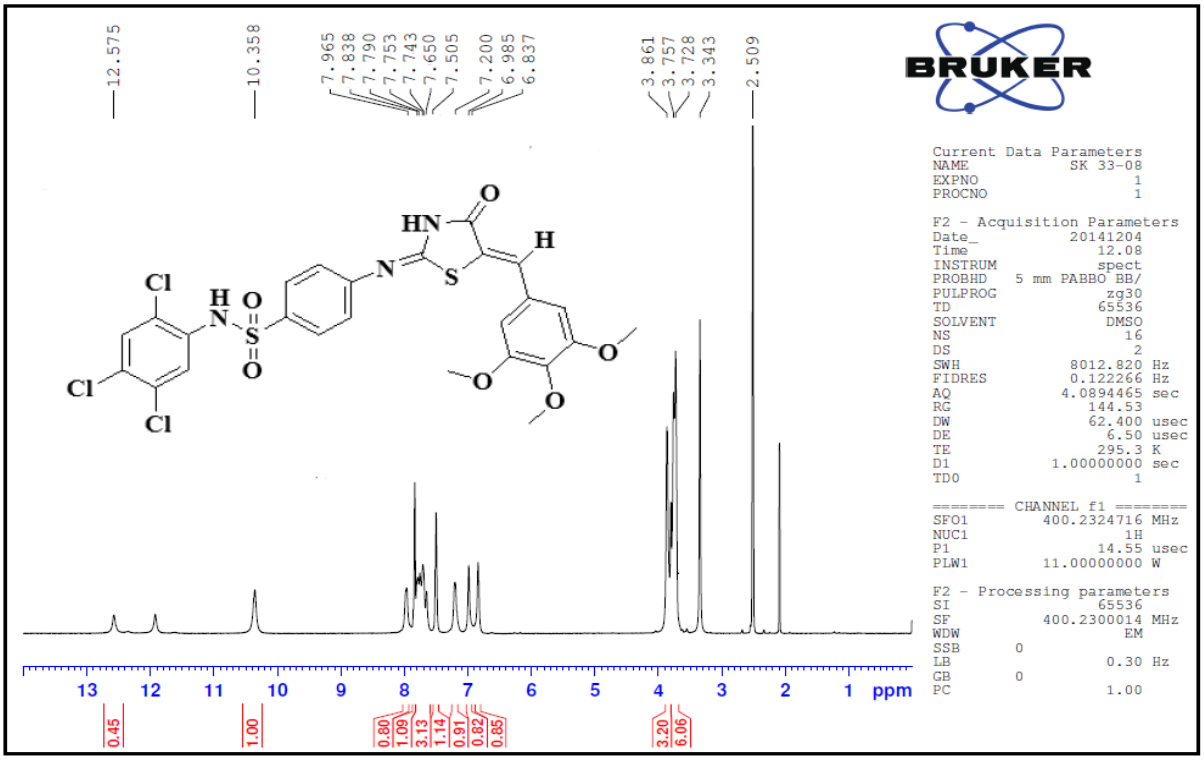

Fig. S28 ^{1}H NMR spectrum of compound **7f**.

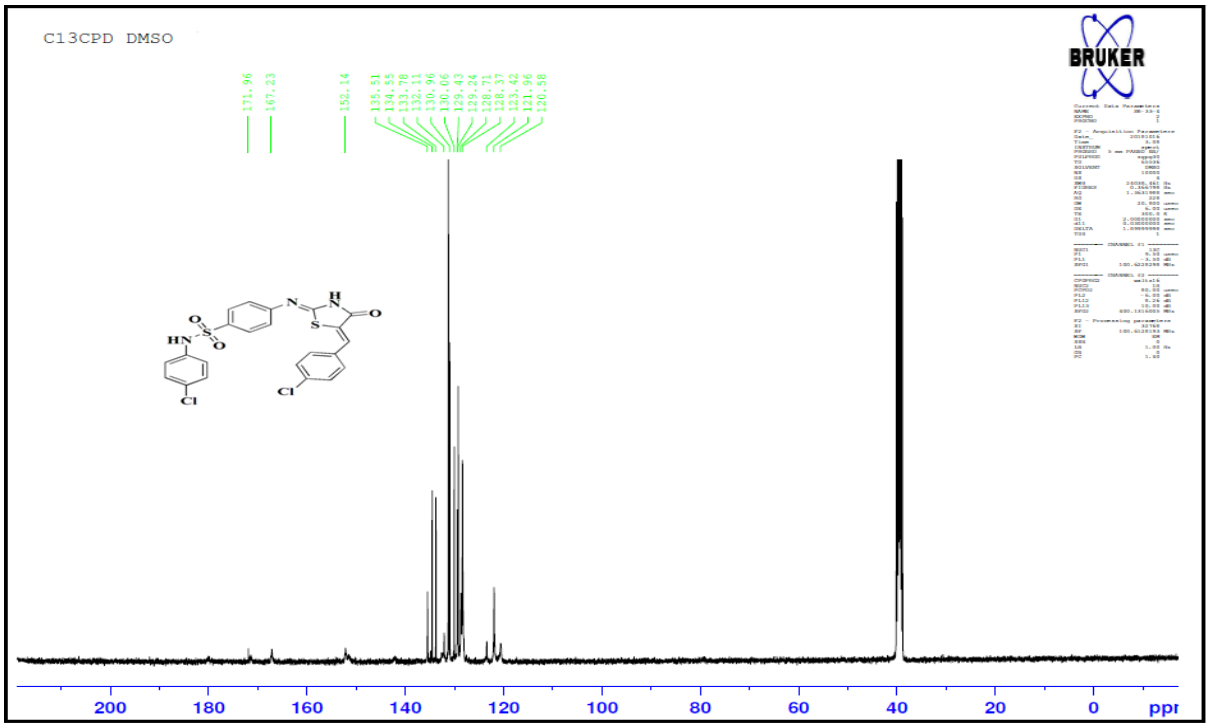

Fig. S29 ^{13}C NMR spectrum of compound **6d**.

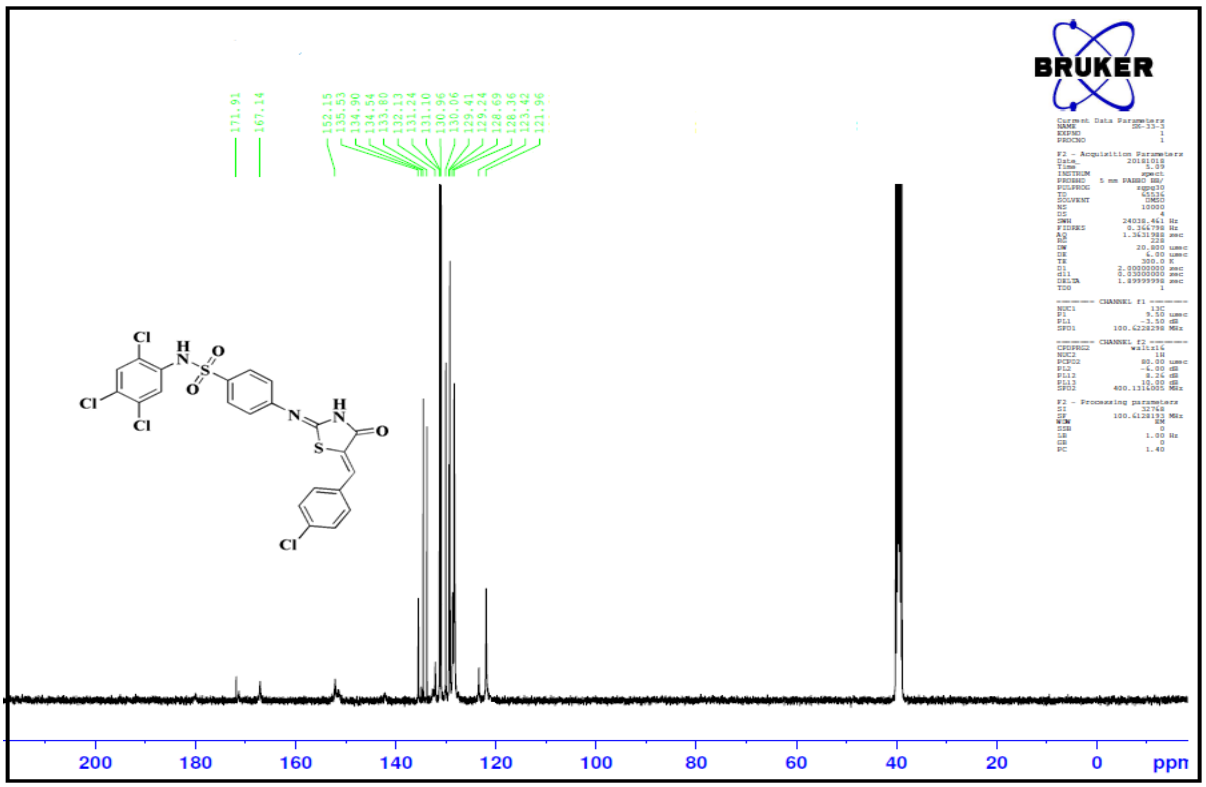

Fig. S30 ^{13}C NMR spectrum of compound **6i**.

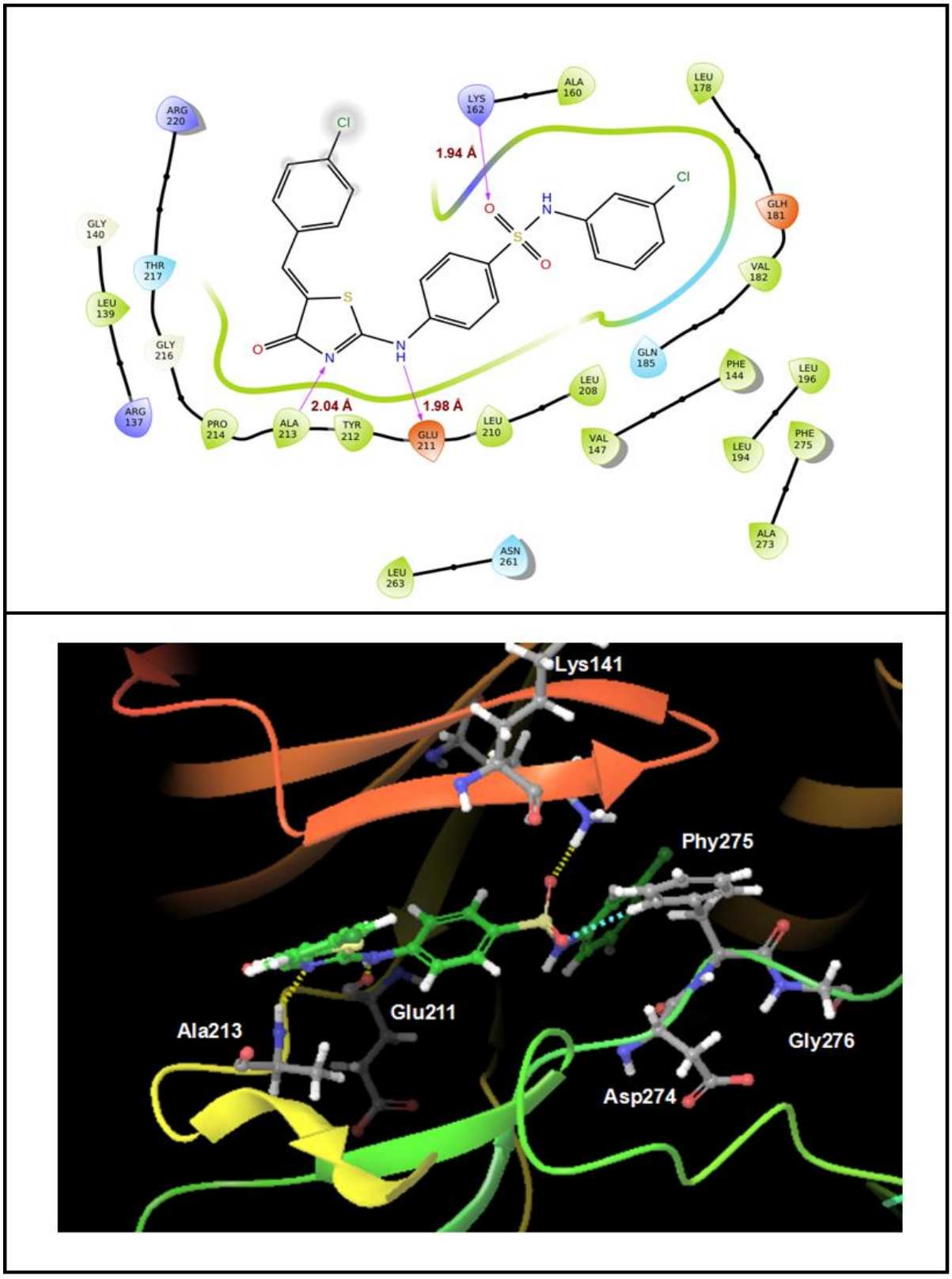

Fig. S31 2D and 3D Docking poses for compound **6c** with AK.

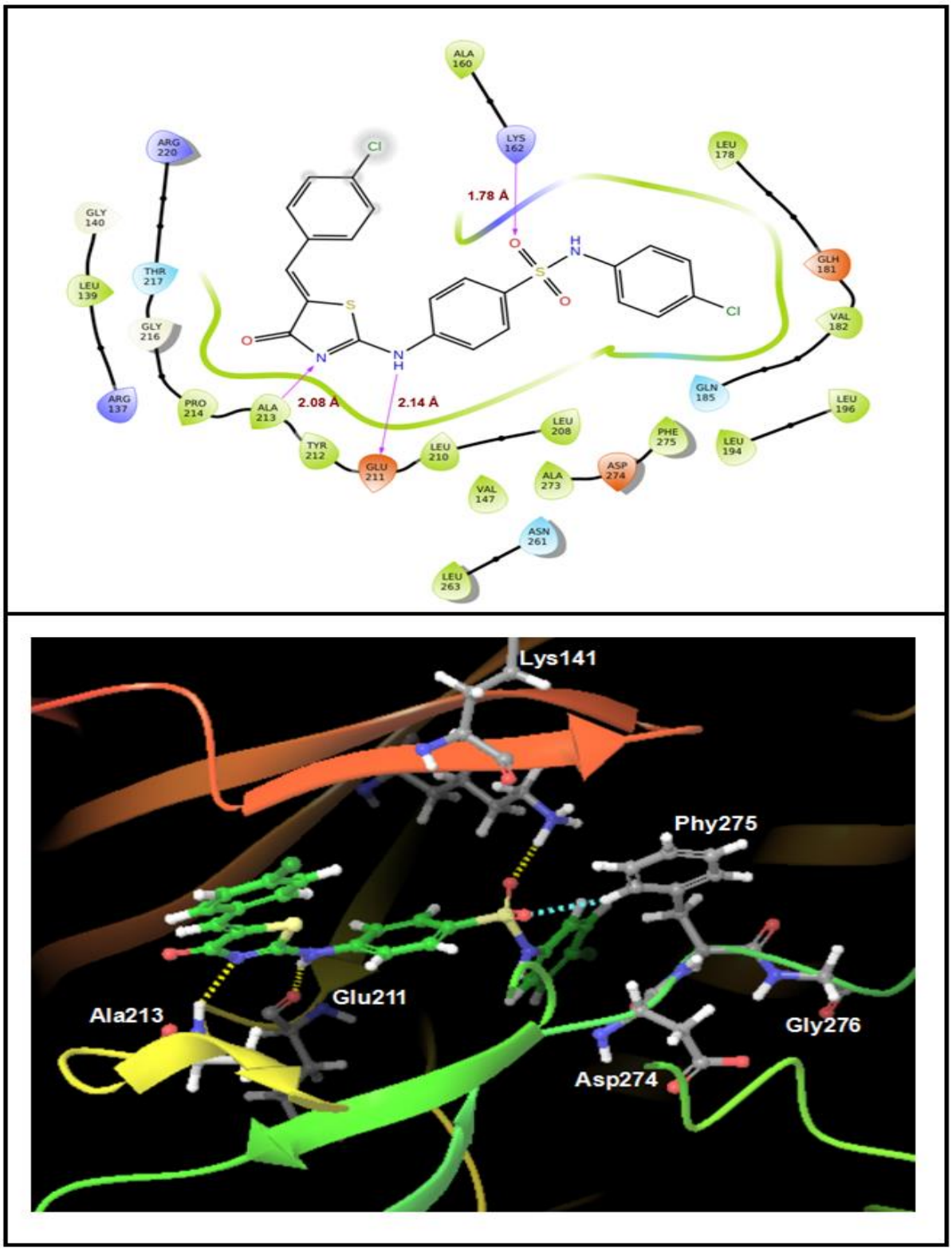

Fig. S32 2D and 3D Docking poses for compound **6d** with AK.

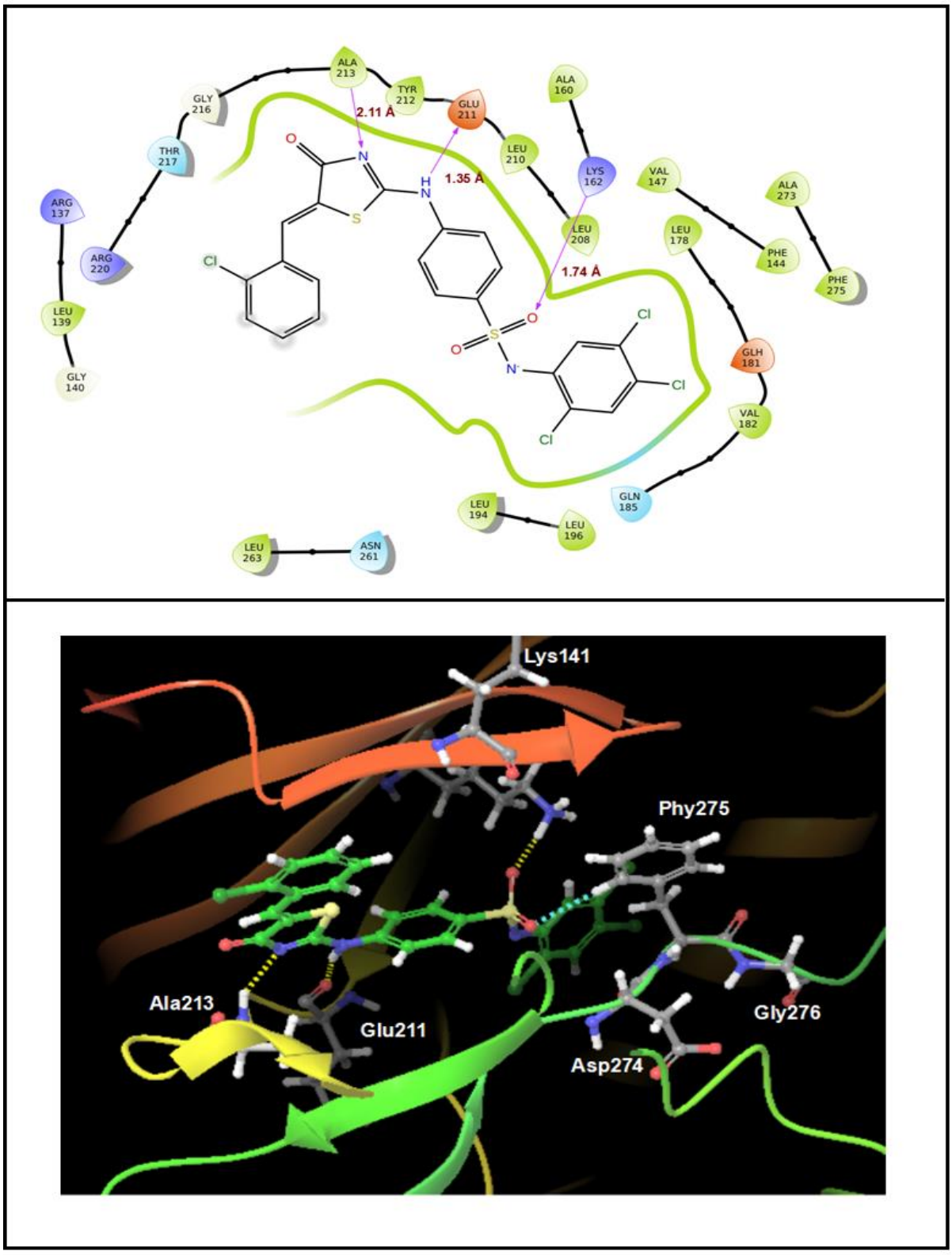

Fig. S33 2D and 3D Docking poses for compound **7b** with AK**.**

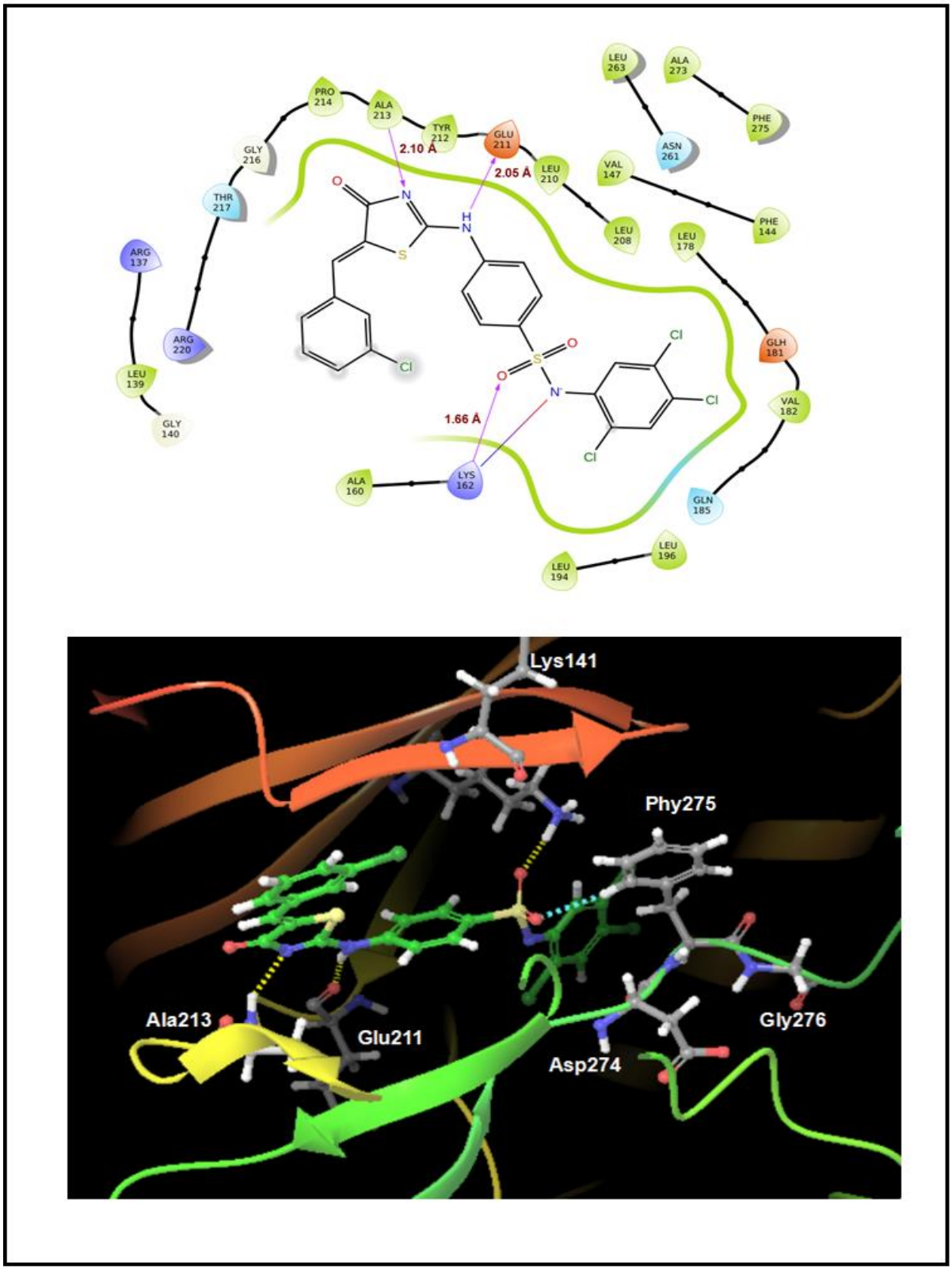

Fig. S34 2D and 3D Docking poses for compound **7c** with AK**.**

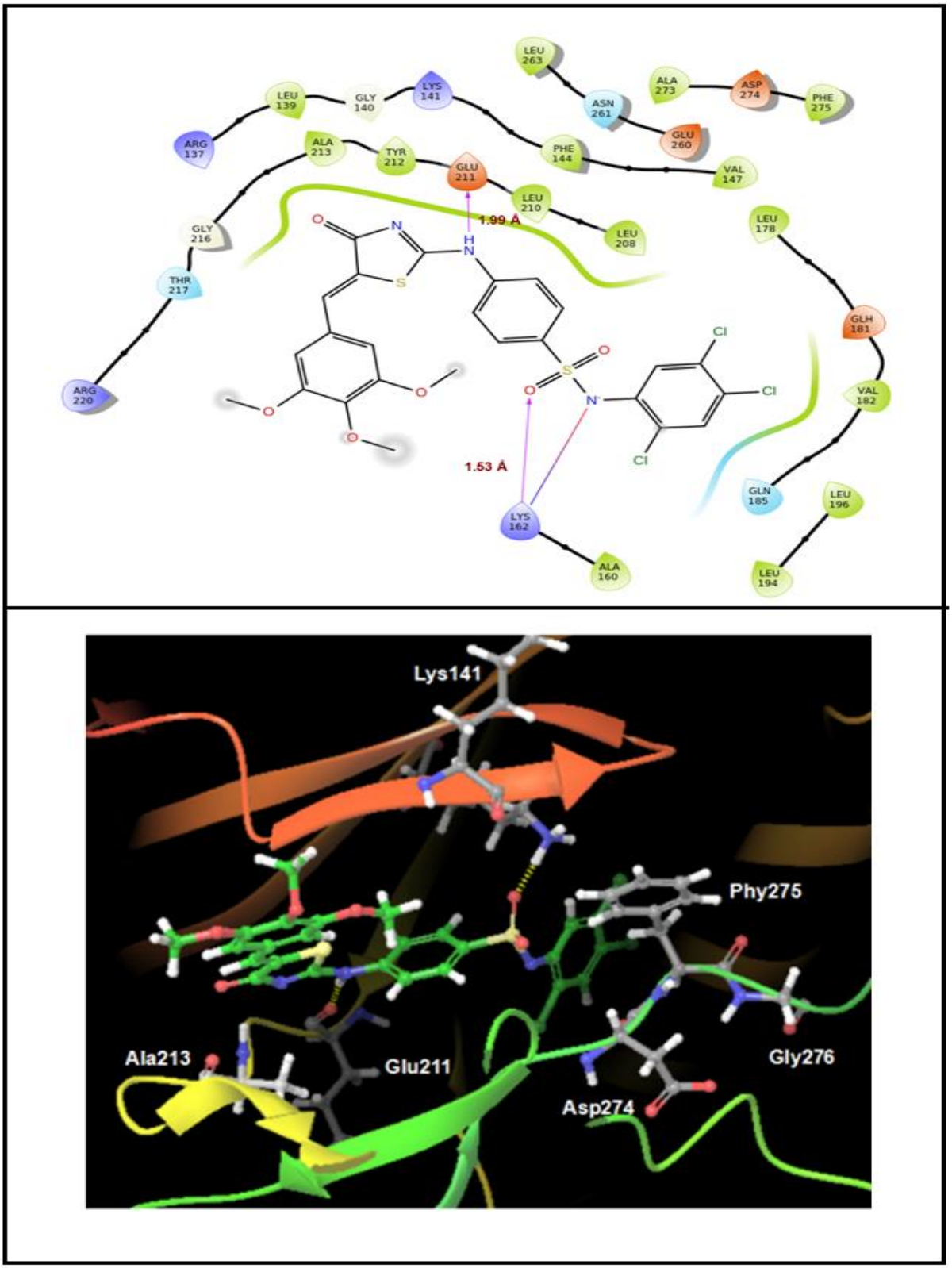

Fig. S35 2D and 3D Docking poses for compound **7f** with AK.